

AN SCR CYCLOCONVERTER FOR A CRYOGENIC
PROPULSION SYSTEM

Scott Lowrie Sears

AN SCR CYCLOCONVERTER FOR A CRYOGENIC PROPULSION SYSTEM

by

SCOTT LOWRIE SEARS

B.S., United States Naval Academy
(1966)

SUBMITTED IN PARTIAL FULFILLMENT

OF THE REQUIREMENTS FOR THE

DEGREE OF MASTER OF

SCIENCE

at the

MASSACHUSETTS INSTITUTE OF TECHNOLOGY

July, 1970

AN SCR CYCLOCONVERTER FOR A CRYOGENIC PROPULSION SYSTEM

by

SCOTT LOWRIE SEARS

Submitted to the Department of Electrical Engineering on July 29, 1970 in partial fulfillment of the requirements for the Degree of Master of Science.

ABSTRACT

The purpose of this thesis was to design the electronic circuitry necessary to operate a thyristor network as an a.c. to a.c. frequency changer, or cycloconverter. A low-power model of an SCR cycloconverter of the configuration proposed for supplying variable-frequency, three-phase, a.c. power to a synchronous ship-propulsion motor with a superconducting field winding was designed. The model was constructed for single phase to single phase operation, and demonstrated speed and torque control of a.c. synchronous motors. Additionally, a direct-coupled low frequency reference signal generator was designed and constructed which generates a three-phase sinusoidal signal of constant amplitude that is spatially dependent on the rotor position. This ensures constant synchronism of the rotor with the stator field, and allows the motor to start synchronously.

THESIS SUPERVISOR: Herbert H. Woodson

TITLE: Philip Sporn Professor of Energy Processing

ACKNOWLEDGEMENTS

I wish to express my gratitude to all those who helped in the preparation of this thesis. Specifically, my thesis supervisor, Professor Herbert H. Woodson, encouraged me throughout the project, and gave me invaluable insight and guidance into the basic theory. Mr. Richard F. Challen, a doctoral candidate, rendered valuable assistance in some phases of electronic design.

I would also like to express my appreciation to the United States Navy, which is sponsoring my education at M.I.T. under the auspices of the Junior Line Officer Advanced Scientific Educational (BURKE) Program.

Finally, I thank my wife, Sharon, for her patience and understanding during the completion of this project.

TABLE OF CONTENTS

Abstract.	2
Acknowledgements.	3
List of Figures	5
List of Tables.	7
Introduction.	8
Chapter I Design Approach.	19
1.1 Single Phase Rectifier Theory	19
1.2 Three Phase Rectifier Theory.	28
1.3 Inverter Operation.	40
1.4 Cycloconverter Application.	41
1.5 Three Phase Low Frequency Generation.	55
Chapter II Design Applications and Circuits.	59
2.1 Cycloconverter Section.	59
2.1.1 Triggering Network	59
2.1.2 Thyristor Network.	72
2.2 Low Frequency Reference Generation.	75
Chapter III Analysis of Performance.	80
Chapter IV Conclusions	88
Appendix A Derivations	96
Appendix B Settings.	102
References.	104

LIST OF FIGURES

<u>Figure</u>	<u>Title</u>	<u>Page</u>
1	Three Phase to One Phase Full Wave Cycloconverter	15
2	Waveform of Envelope Cycloconverter	17
3	Half Wave Rectifier	20
4	Full Wave Rectifier	20
5	Current in Half Wave Rectifier	24
6	Variation of Average Voltage and RMS Current with Thyristor Firing Angle for a Resistive Load	25
7	Full Wave Thyristor Rectifier	27
8a	Half Wave Bridge	30
8b	Full Wave Bridge	30
9a	Three Phase Full Wave Bridge Rectifier	33
9b	Full Wave Rectifier Waveform	33
10a	Hybrid Bridge Circuit	35
10b	Complete Bridge Circuit	35
11	Three Phase Half Wave Rectifier	38
12	Single Phase to Single Phase Cycloconverter	48
13	Ramp Circuit	61
14	Waveforms in Ramp Circuit	63
15	Summing Circuit	65

16	Waveforms of Summing Circuit	66
17a	Sign Detectors	67
17b	Logic Section	68
18	Pulse Circuit	70
19	Trigger Circuit	71
20	Motor Drive Circuit	73
21a	Demodulator Circuit	76
21b	Filter Circuit	77
22	Resistive Load Voltage	81
23	Firing Pulses	81
24	Voltage and Current in Inductive Load	83
25a	Motor at 180 RPM	85
25b	Motor at 450 RPM	85
26	Cycloconverter Control System	89
27	Proposed Speed Control	93

LIST OF TABLES

<u>Table</u>	<u>Title</u>	<u>Page</u>
1	Truth Table	49
2	Karnaugh Maps	51
3	Modified Truth Table	53

INTRODUCTION

The design of a specific propulsion system has in the past been predicated upon optimum use of available system components to a large degree. The limitations of this approach are obvious. In any naval propulsion system, present equipment soon reaches optimum levels of utilization, and in order to significantly improve the performance of a vessel, a new, perhaps radical, approach must be employed. The new design concepts must be, however, of such a significant improvement over existing systems that the expense and development of the new system can be economically warranted.

A design engineer is ordinarily given a requirement that a new design must fulfill. In propulsion systems, the requirements are in terms of speed and power. It is the task, then, of the engineer to meet these requirements while optimizing other standards. In the past, the engineer has attempted to minimize weight and volume of propulsion systems, while maximizing fuel economy and reliability. Even these four criteria often demand trade-offs in order to

optimize the entire system. Unfortunately, at the same time, other aspects, such as system response, flexibility to meet other requirements and stability have simply been ignored until after the improved system has been designed. These aspects are then determined, and consequently remain system limitations, as a consequence of the system design.

Historically, naval propulsion systems have consisted of boiler-turbine-reduction gear drive systems. When an increased speed or power requirement is determined for a new design of vessels, improvements are made in this basic drive system. Improvements have been significant -- the development of 1200 pound steam systems, nuclear reactors to provide the thermal energy in the boilers, and high speed turbines -- which have led to drive systems of high performance and good economy. Electric drive systems have, in general, been developed for small vessels only, such as diesel-electric submarines and small auxiliary vessels. These drive systems for the most part employ large d.c. motors.

Conventional d.c. machines are limited in size because of the difficulties in extracting large amounts of

power from the rotating armature. Investigations into new d.c. machine designs, such as the homopolar machines, have been conducted, but homopolar machines, being low-voltage, high-current machines, tend to be quite lossy at the current extraction points under heavy loads.

A.c. machines in the past have been considered too large and heavy for their power requirement to be used in naval propulsion systems. However, significant progress has been made in the development of new a.c. synchronous machines with superconducting field windings, which have the advantage of significantly reducing the weight and volume for equivalent power output, while at the same time -- increasing the system response over conventional propulsion systems.¹ A.c. machines have an immediate advantage over similar d.c. machines in large power applications, since the only current which must be applied to the rotating field is excitation current, which is normally only a small fraction of the armature current. Thus, the high current collection problems are avoided, since most of the current is applied directly to a stationary armature.

If a.c. synchronous machines are selected as the basis of a new propulsion system, radical changes must be made in the area of power controllers. In conventional boiler-turbine systems, control is maintained by direction and flow rate through steam turbines. Even in d.c. machine propulsion systems, system control can be maintained by control of field current or armature voltage to yield constant horsepower or constant torque as desired. The control of an a.c. machine is not so simple. An a.c. synchronous machine must be rotating at a synchronous speed determined by the frequency of the line power supplied to it in order to deliver torque. If the synchronous machine is to be directly attached to the propulsion shaft, shaft speed can only be controlled by the control of the line frequency of the a.c. power being delivered to the armature of the machine. The amount of torque at any given speed then can be controlled by controlling the magnitude and phase of the armature current. Thus the power controller must be able to control one or both of these current functions.

In order to provide smooth continuous torque to the propulsion shaft, the motor must be polyphase; standard synchronous motors tend to be normally two or three phase. Thus the power controller must be able not only to supply a variable frequency current to the motor, but must also provide three or six phase current whose phase relationship is constant over the entire frequency range of the power supplied. In order to reverse the motor, the power controller must be able to reverse this phase relationship, and must allow for reverse flow through it to provide for regenerative braking.

The solid state frequency converter which is flexible enough to meet all of these requirements is a cycloconverter. A cycloconverter is a form of a.c. to a.c. frequency changer, employing controllable rectifiers. It differs from other solid state a.c. to a.c. frequency changers, such as rectifier-inverter combinations, in that there is no d.c. link, where no reactive power may be transmitted. In other conventional solid state frequency changers, reactive power must be added to the load circuit through either tuned storage elements (capacitors or inductors) or through a large synchronous condenser unless

the synchronous motor is always run at unity power factor. The high power levels required by a propulsion motor eliminate the possible use of capacitors, and in order to drive the machine at unity power factor, the excitation current must be controlled.

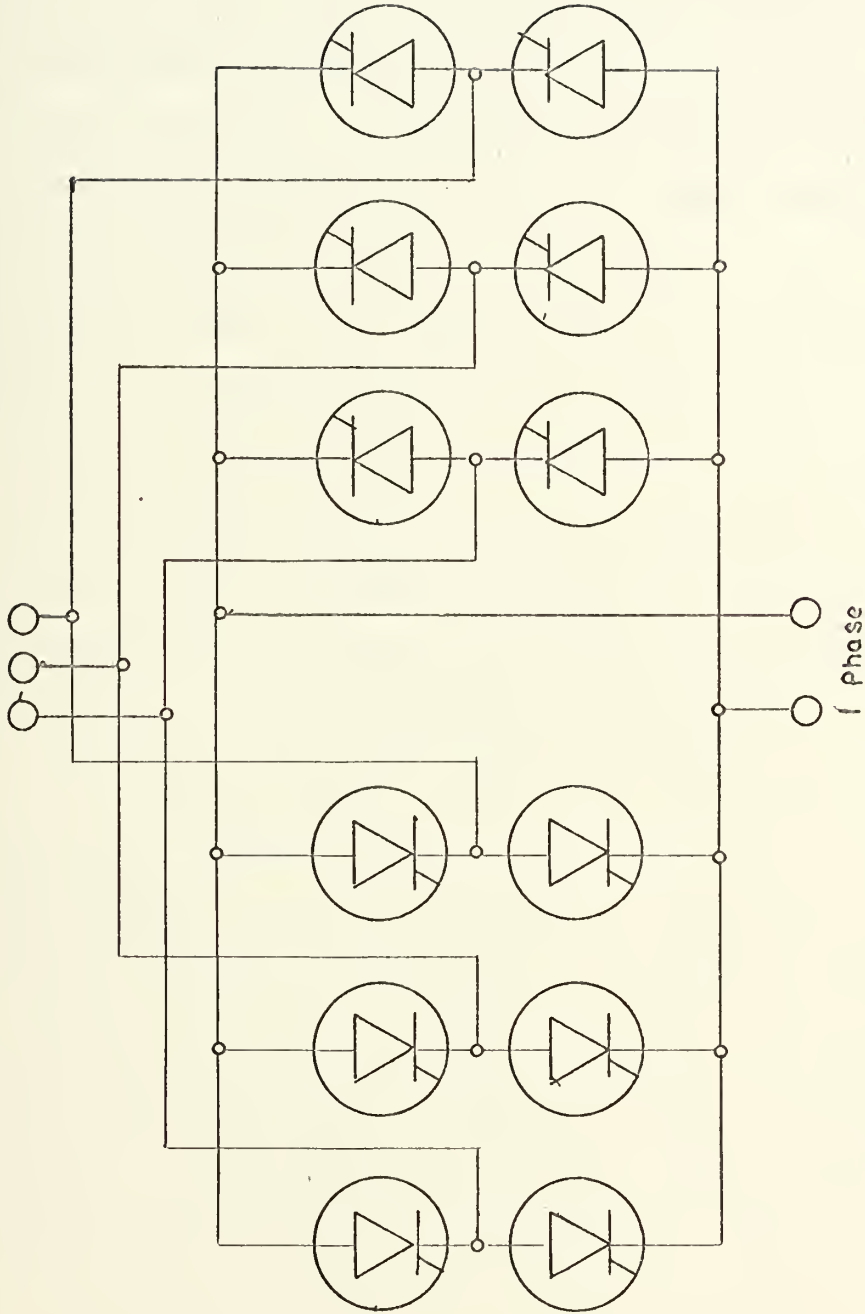
"Cycloconversion" is the term generally applied to using an a.c. input of one fixed frequency, and electronically "chopping" the waveform so as to assimilate a lower frequency a.c. waveform (as opposed to "cycloinversion", which changes the fixed frequency to a higher output frequency). The term "cycloconverter" was originated by the Germans in the 1930's to specify devices employing mercury arc rectifiers, used to convert three phase, 50 hertz source power to a single phase, $16 \frac{2}{3}$ hertz supply for a.c. traction used by the German State Railways.^{2,3} The advent of semiconductor silicon controlled rectifiers has added new impetus to the development of cycloconverters, because of their significant advantages. The new silicon controlled rectifiers differ from the earlier mercury arc rectifiers in that the former are fired by application of gate current, while the latter are controlled by grid voltage. These semiconductor devices have

significant advantages over the mercury arc rectifiers in size, power range, and most importantly, price.

A basic cycloconverter circuit consists of a pair of conventional a.c. to d.c. rectifier circuits connected in parallel, as shown in figure 1. The groups are designated as positive and negative, as determined by the direction of current conduction. Early concepts in cycloconverters proposed merely firing the positive and then the negative groups sequentially at the desired frequency.³ This method of cycloconversion, designated envelope cycloconversion, was then simply a controlled rectifier in which the rectified current was alternating between positive and negative d.c. values. All commutation between current carrying rectifiers was natural, and no grid control was needed to vary the angle of firing. The major drawbacks were that the envelope cycloconverter could only supply noninductive loads, and that no energy regeneration backwards through the cycloconverter was possible.

Rissik, then, was responsible for the development of the "grid-controlled cycloconverter," so named because

3 Phase

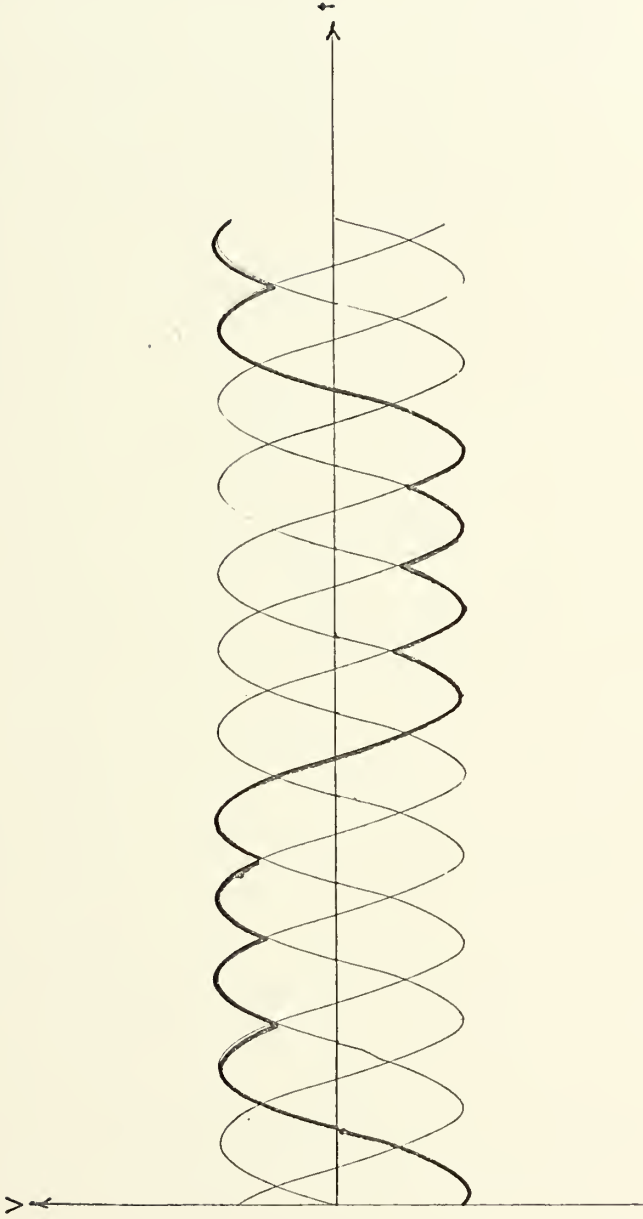


Three Phase to One Phase Full Wave Cycloconverter

Figure 1

the mercury arc rectifiers were controlled by adjusting the grid voltage. The low frequency signal in this case is generated by controlling the firing angle of the controlled rectifiers. By sinusoidally varying the firing angle of the conducting rectifier, the output waveform is approximately sinusoidal (see Section 1.4). The harmonic content of the output waveform is greater than that of the envelope cycloconverter (figure 2), but it has the advantage of power regeneration and flexibility to be connected to loads requiring any power factor. In order to reduce the harmonic distortion, a full wave cycloconverter, which uses both positive and negative cycles, as in a full wave rectifier, is desirable.

The cycloconverter can supply power over a continuous frequency range from zero hertz (d.c.) to approximately one third the frequency of the input voltage. Whereas reactors were used in the early models of cycloconverters to limit the circulating currents caused by providing firing pulses to banks of rectifiers, positive control of the firing signal is used to blank possible inter-circuit shorts. The cycloconverter, using this



Waveform of Envelope Cycloconverter

Figure 2

technique, becomes an efficient, practical method of frequency conversion with direct application for speed control of a.c. machines.

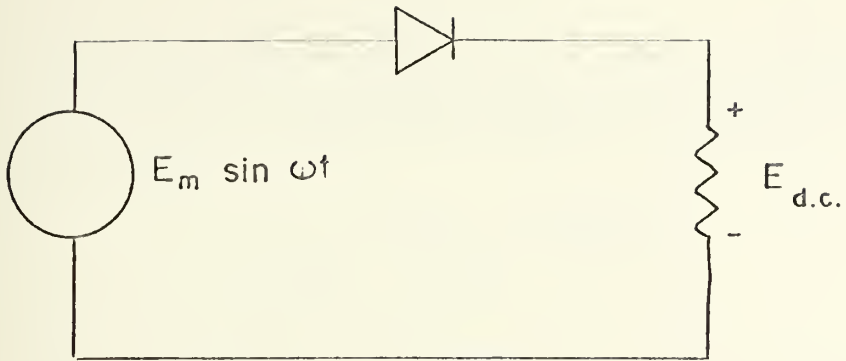
Chapter I

Design Approach

The analysis of the cycloconverter operation can best be understood if subdivided into its fundamental components. There are two basic sections to the cycloconverter. The first section is the conduction section, consisting of the basic arrangement of thyristors shown in figure 1. The theory of operation of thyristors can be shown from first a basic look at diode rectifier waveforms, followed by analysis of the results of controlling the firing angle. The second section to be examined is the firing control circuitry, most often given in the literature as a "black box." This is the heart of the cycloconverter operation. A subsidiary section, but nevertheless important for the application to propulsion systems, is the generation of the three phase variable frequency reference signal.

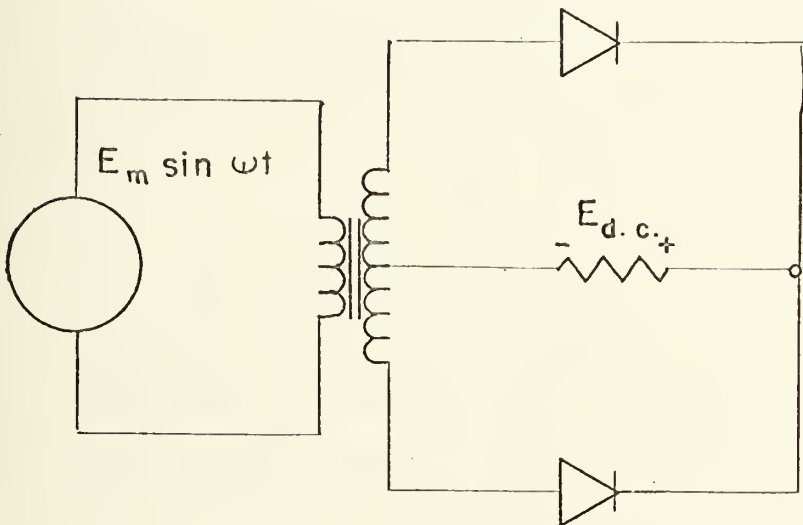
1.1 Single Phase Rectifier Theory

Consider the basic diode rectifier, resistive load circuit of figure 3. To determine the average value



Half Wave Rectifier

Figure 3



Full Wave Rectifier

Figure 4

of voltage across the load, the voltage is integrated over half of a cycle, and divided by the period of the wave form.

$$E_{d.c.} = \frac{E_m}{\pi} = 0.318 E_m \quad (1.1.1)$$

E_m refers to the peak instantaneous value of voltage, rather than RMS voltage. The derivations are shown in Appendix A. For a strictly resistive load, the average value of the load current is the average d.c. value of voltage divided by the load resistance.

$$I_{d.c.} = \frac{E_m}{\pi R} = 0.318 \frac{E_m}{R} \quad (1.1.2)$$

In order to determine the heating value of the load current, the RMS current can be determined.

$$I_{RMS} = \frac{E_m}{2R} \quad (1.1.3)$$

Figure 4 shows the single phase diode rectifier, resistive load circuit operating as a full wave rectifier. Obviously, the average value of voltage and RMS current will increase. The d.c. value of voltage will double.

$$E_{d.c.} = \frac{2E_m}{\pi} \quad (1.1.4)$$

The RMS value of current does not double, but only increases by the square root of 2.

$$I_{\text{RMS}} = \frac{\sqrt{2} E_m}{2R} \quad (1.1.5)$$

The effectiveness of power can be measured by the ratio of the average power (power used in the generation of torque) to the RMS value of power (which is the source of heating). Therefore, in addition to delivering a smoother waveform, the full wave rectifier is more effective in delivering power to a load.

Controlled output may be achieved by connecting SCR's, which are also called thyristors, into the circuits discussed above in place of the conventional diodes. SCR's are semiconductor devices, which block current in both directions, unless a firing pulse is applied to the gate of the device, in which case it will pass forward current, as long as the current level exceeds a minimum holding current, with only a voltage drop of approximately one volt across the junction.⁴

The analysis of the half wave circuit with thyristors differs from the diode rectifier circuit only

in the addition of the firing angle α as a variable. Current will be in the load now only between $\omega t = \alpha$ and $\omega t = \pi$ (figure 5). The expression for the average value of voltage across the load is

$$E_{d.c.} = \frac{E_m}{2\pi} (1 + \cos \alpha) \quad (1.1.6)$$

This will equate to equation (1.1.1) when $\alpha = 0$. Similarly,

$$I_{RMS} = \frac{E_m}{2\sqrt{\pi} R} (\pi - \alpha + \frac{1}{2} \sin 2\alpha)^{1/2} \quad (1.1.7)$$

which, when $\alpha = 0$, reduces to equation (1.1.3). The variations of these equations are plotted in figure 6.

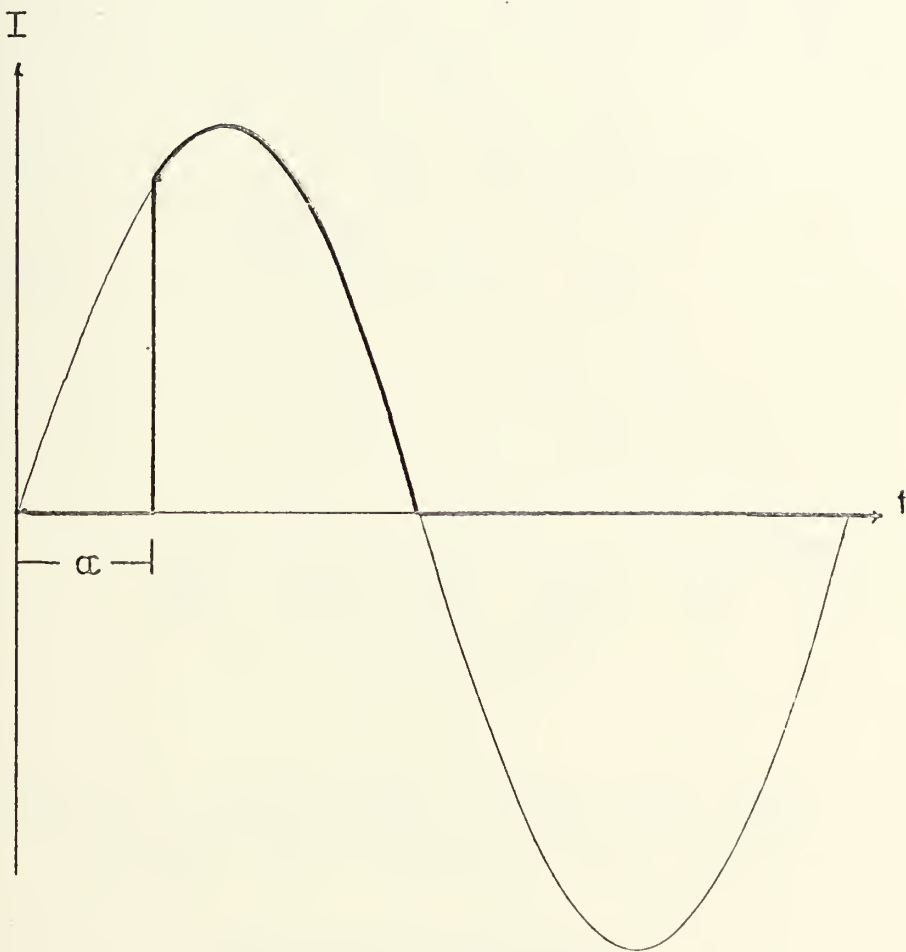
If thyristors are used in the case of full wave circuits in place of the diodes, similar analysis shows that

$$E_{d.c.} = \frac{E_m}{\pi} (1 + \cos \alpha) \quad (1.1.8)$$

and

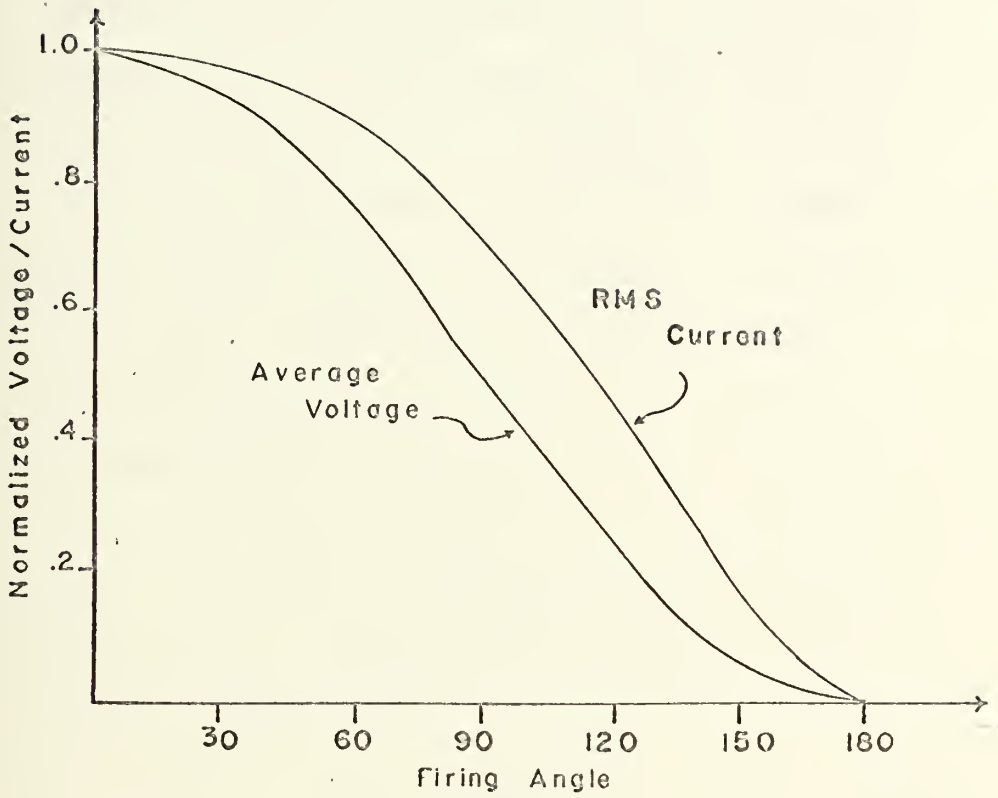
$$I_{RMS} = \frac{E_m}{\sqrt{2\pi} R} (\pi - \alpha + \frac{1}{2} \sin 2\alpha)^{1/2} \quad (1.1.9)$$

These equations are not developed in Appendix A, for they follow directly from previous development.



Current in Half Wave Rectifier

Figure 5



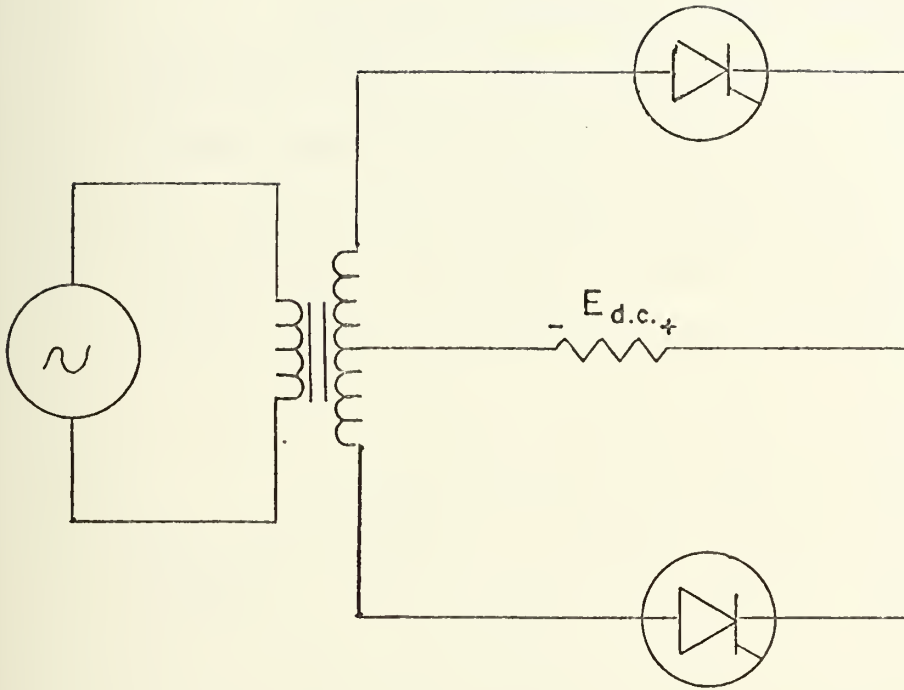
Variation of Average Voltage and RMS Current with Thyristor Firing Angle for a Resistive Load

Figure 6

Unfortunately, most realistic loads are inductive as well as resistive, which complicates the expressions for the load voltage. Assume that in the circuit of figure 7, the load current is continuous; that is, the firing angle of the thyristor is small enough that an average d.c. current must be delivered to the load. In this case, each SCR will continue conducting current until the firing of the opposite SCR causes natural commutation. From α to π , the SCR will deliver positive power to the load, and between π and $\pi + \alpha$, it will deliver negative power to the load. The average d.c. voltage across the inductive load can then be calculated to be

$$E_{d.c.} = \frac{2E_m}{\pi} \cos \alpha \quad (1.1.10)$$

This means that the average d.c. voltage delivered to the load is positive for firing angles of less than 90 degrees, but negative for firing angles of greater than 90 degrees. This shows the ability of thyristor circuits to feed back energy to the supply in the case of inductive loads. A diode bridge circuit, characterized by $\alpha = 0$, cannot perform this.



Full Wave Thyristor Rectifier

Figure 7

1.2 Three Phase Rectifier Theory

In order to improve the output waveform of any rectifier network, polyphase operation is desirable. In current power technology, three phase power sources are most common, because of their maximum economy in transmitting power. Therefore, most power generation developments have been in the area of three phase systems.

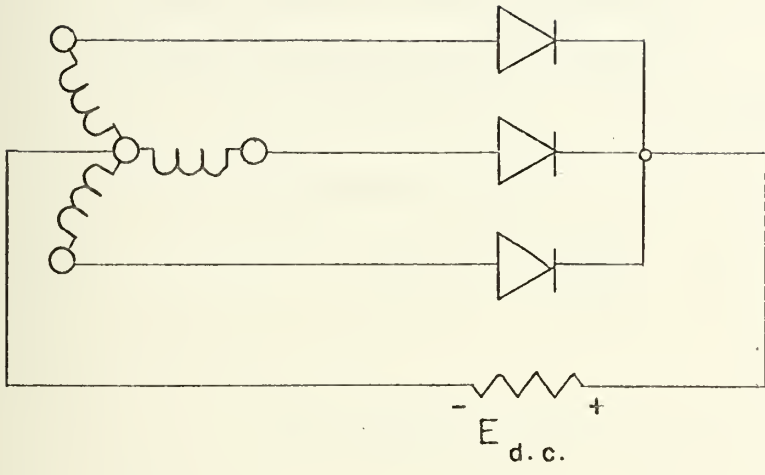
Three phase rectifier circuits can be divided into two basic types -- half wave bridges and full wave bridges.⁵ Full wave bridges are often sub-classified into complete and incomplete bridges; an incomplete bridge is a hybrid bridge consisting of half thyristors and half diodes. A half wave bridge is obviously less expensive for it requires only half the diodes or thyristors required by a full wave bridge, and, in the case of a thyristor bridge, only half the number of timing circuits required by a full wave bridge. It does, however, have the disadvantage of having a more discontinuous waveform, and of requiring a neutral or return path to the supply, necessitating a wye connected transformer.

A typical half wave three phase diode bridge network is shown in figure 8a. Assume that the load is resistive and returns to a common neutral, such as the star connection of a transformer. Each rectifier conducts only for one third of a cycle -- from $\pi/6$ to $5\pi/6$ in its own reference frame. Through natural commutation, each diode conducts while its line voltage is greater than the other two. As can be seen in figure 8b, the output wave form has an average value with an a.c. ripple on top having fundamental component of frequency equal to triple the line frequency.

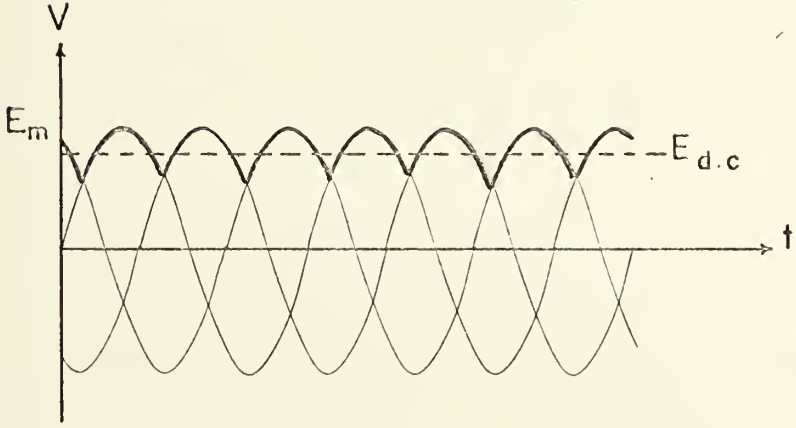
The average value of the d.c. voltage across the load is equal to

$$E_{d.c.} = \frac{3\sqrt{3}}{2\pi} E_m = 0.827 E_m \quad (1.2.1)$$

If the diodes are replaced by thyristors, the firing angle of operation can only be controlled between $\pi/6$ and π (with a resistive load). If the firing pulse is terminated before or commenced after this range, then the thyristor will block the entire time. The angle α is



Half Wave Bridge
Figure 8a



Load Voltage
Figure 8b

measured from the value of ωt which produces the maximum value of load voltage, $E_{d.c.}$. In the case of three phase half wave operation, $E_{d.c. \max}$ occurs at $\omega t = \pi/6$, at which point $\alpha = 0$. For $\alpha = 0$ to $\alpha = \pi/6$, there is continuous current in the load resistor.

$$E_{d.c.} = \frac{3 \sqrt{3} E_m}{2\pi} \cos \alpha \quad (1.2.2)$$

For α greater than $\pi/6$ and less than $5\pi/6$, the conduction is discontinuous for resistive loads. The average value of d.c. voltage is then given by

$$E_{d.c.} = \frac{3 E_m}{2\pi} [1 + \cos (\alpha + \pi/6)] \quad (1.2.3)$$

In the most general case, for any polyphase half wave bridge circuit, the average load voltage can be expressed as

$$E_{d.c.} = \frac{n E_m}{\pi} \sin \frac{\pi}{n} \cos \alpha \quad (1.2.4)$$

where n is the number of phases in the circuit. This equation is applicable for the case of continuous conduction of current only. As the number of phases increases, the "critical" angle, past which there is discontinuous conduction, decreases. In general, the

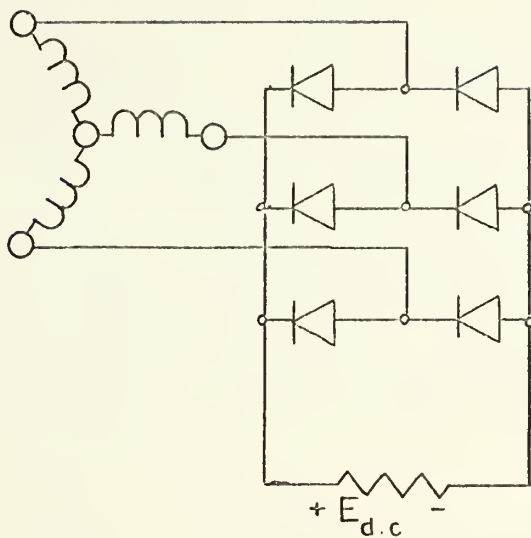
critical angle α_c is given as

$$\alpha_c = \frac{\pi (4 - n)}{2n} \quad (1.2.5)$$

where n is the number of phases.

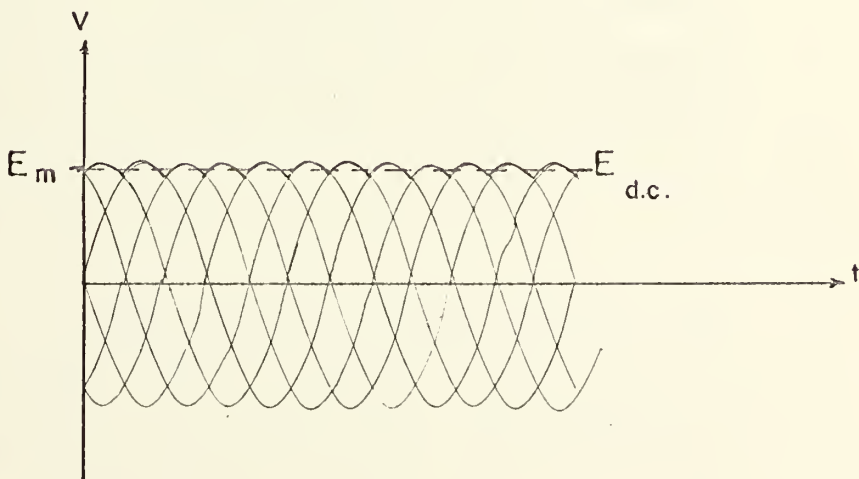
The three phase full wave bridge is a more complex circuit to analyze in terms of individual thyristor operation. Figure 9 is a representation of a typical circuit and its accompanying waveform, for the case of diode rectifier elements. For a resistive load, the load voltage corresponds to the maximum $\pi/3$ portions of the three phase input voltages. Each diode will conduct for a total of one third of a cycle, but half of this time it is acting as the return path for the current to the source. Therefore, the output waveform has an average d.c. value with an a.c. ripple superimposed on top having a fundamental component of frequency equal to six times the line frequency.

The full wave bridge circuit yields the maximum d.c. value of any three phase rectifier circuit. The average value of the d.c. voltage across



Three Phase Full Wave Bridge Rectifier

Figure 9a



Full Wave Rectifier Waveform

Figure 9b

the load is equal to

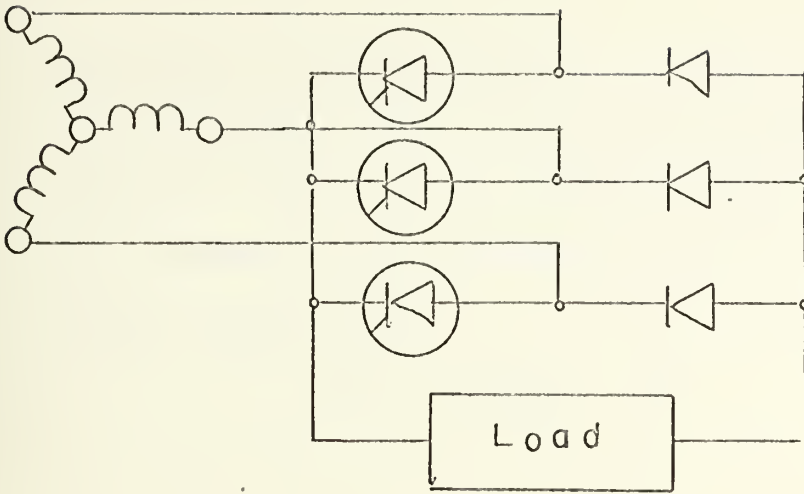
$$E_{d.c.} = \frac{3 E_m}{\pi} = 0.955 E_m \quad (1.2.6)$$

In this case, E_m is the peak line-to-line voltage. If this value is compared to the half wave bridge, it should be converted in terms of line-to-neutral voltages. In this case

$$E_{d.c.} = \frac{3 \sqrt{3} E_m}{\pi} = 1.654 E_{m_{l-n}} \quad (1.2.7)$$

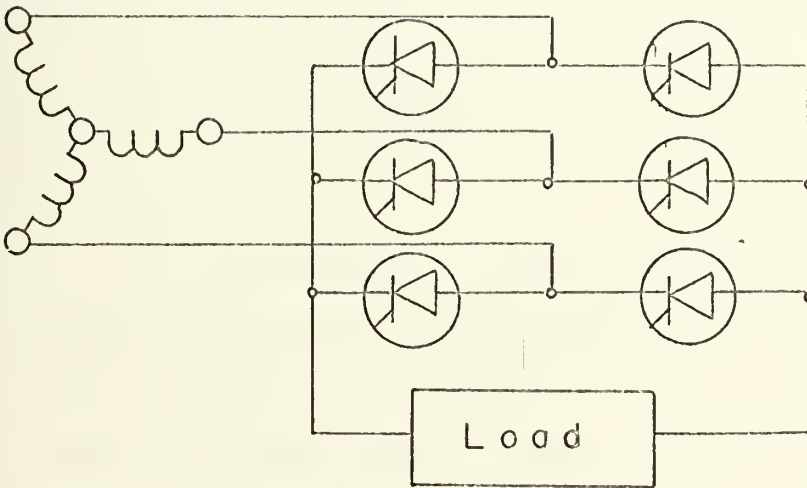
It was indicated earlier in the chapter that the diodes could be replaced in two basic ways in the full wave bridge network (in actual circuitry, there may be five or more variations, but only two are standardized⁴). In the incomplete full wave thyristor bridge, the diodes used in half of the network are replaced by thyristors (figure 10a). The complete full wave bridge consists of six thyristors (figure 10b).

With thyristors in place of diodes, the firing angle again is measured from the value of ωt producing maximum load voltage, which in this case is $\omega t = \pi/3$. Therefore, for resistive loads, the firing



Hybrid Bridge Circuit

Figure 10a



Complete Bridge Circuit

Figure 10b

angle must be controlled between $\alpha = 0$ and $\alpha = 2\pi/3$ for the full wave bridge circuit (it can be controlled between $\alpha = 0$ and $\alpha = \pi$ for the hybrid bridge circuit). For α greater than 0 and less than $\pi/3$, there is continuous conduction, and

$$E_{d.c.} = \frac{3 E_m}{\pi} \cos \alpha \quad (1.2.8)$$

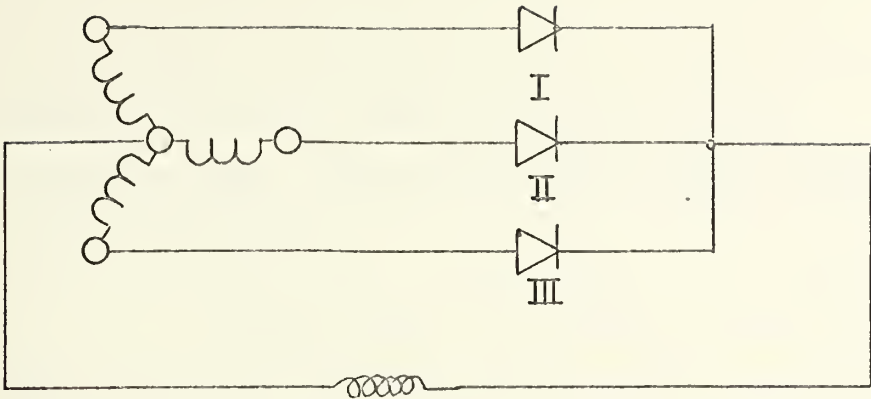
If the firing angle α occurs in the region between $\alpha = \pi/3$ and $\alpha = 2\pi/3$, the first conducting thyristor turns off before the next conducting thyristor turns on, causing discontinuous conduction. The average value of d.c. load voltage is then

$$E_{d.c.} = \frac{3 E_m}{\pi} [1 + \cos (\alpha + \pi/3)] \quad (1.2.9)$$

The analysis of voltage and current relations developed above which are applicable to rectifier systems, are based on a number of simplifying assumptions, such as perfectly resistive loads and ideal supplies -- that is, no inductance exists in either the load or the a.c. supply circuit, which inhibits the phase currents

from instantaneously changing from zero to full value. This implies that there is instantaneous phase commutation.

Any reactance in the a.c. supply will cause current overlapping at the time of phase commutation. Under ideal conditions, all of the current passing through one rectifier is terminated and full current flow through the next conducting rectifier is initiated at the instant of phase commutation without delay (figure 11a). Inductance in the supply to the rectifier both causes the current in the first phase to decay exponentially, and the current in the next succeeding phase to rise exponentially. Thus the succeeding phase commutation is not completed until after a finite interval; the angle of overlap is often designated μ (shown in figure 11b). The more the inductance in the supply circuit, then obviously the greater the amount of distortion in the current shape. Since the two rectifiers are conducting simultaneously, the voltage waveform is also distorted (figure 11c). Since the load voltage is equal to the mean of the two conducting



Three Phase Half Wave Rectifier

Figure II

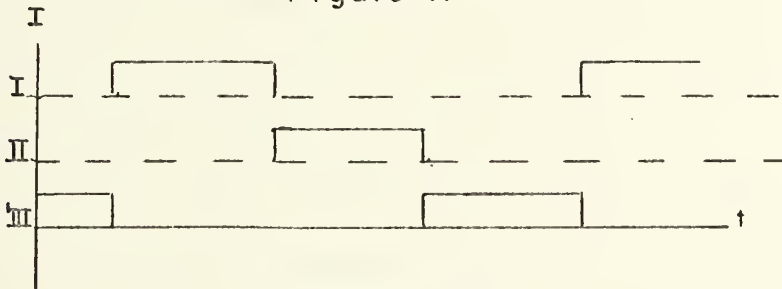


Figure IIa

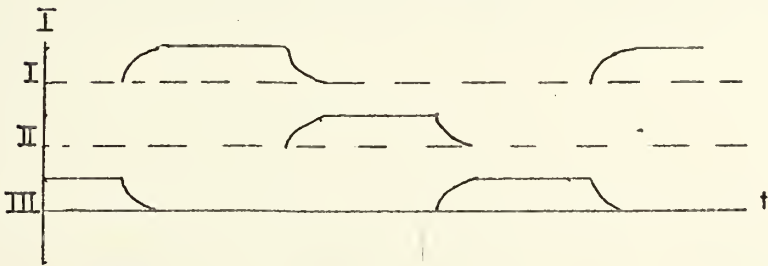


Figure IIb

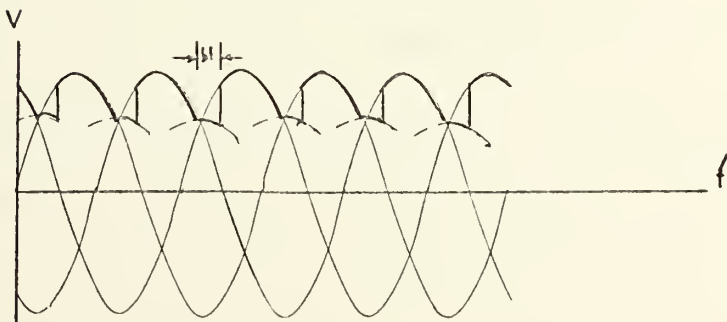


Figure IIc

phases, the overall effect is to reduce the load voltage as shown. The form of the mean output voltage is then reduced to

$$E_{d.c.}' = E_{d.c.} \cos^2 (\mu/2) \quad (1.2.10)$$

The sum of the overlapping phase currents is constant during the commutating period, and is equal to the load current (if, under conditions of infinite load inductance, the load current is constant). Thus the overall effect of input circuit reactance is to increase the current-conducting period of each phase, without altering the maximum value of the load currents or average value of the phase currents, but reducing the mean output voltage. The input RMS current is also reduced.

If the diodes are replaced by SCR's, the voltage reduction is not only proportional to the current overlap μ , but also to the firing angle α .

$$E_{d.c.}' = E_{d.c.} \frac{\cos \alpha + \cos (\alpha + \mu)}{2} \quad (1.2.11)$$

This, of course, reduces to equation (1.2.2) when the overlap interval $\mu = 0$. The same current relations hold

in this case as in the diode case.

1.3 Inverter Operation

In section 1.2, it was shown that there exists a critical angle α_c , beyond which there is discontinuous conduction for noninductive loads. With inductive loads, however, the flow of current can be maintained in the load circuit, and thus in the individual phases of the rectifier network during the interval between voltage zero-crossovers, and the new commutation angle α . During these intervals, the rectifier is supplying energy back to the a.c. supply directly from the load; in other words, it is acting as an inverter. It is evident that the rectifier can only operate in this mode if thyristors are used -- diodes will not suffice.

When defining inversion, the firing angle α is generally not the defining angle, but in its place is the extinction angle β , which is equal to $\pi - \alpha$. The mean output voltage during inversion is then

$$E_{d.c.} = \frac{-3 E_m}{\pi} \cos \beta \quad (1.3.1)$$

There is a finite value of β beyond which inversion cannot take place. The interval $(\beta - \mu)$ is the angle between the completion of the phase commutation $(\alpha + \mu)$ and the point where the phase voltages are equal $(\alpha = \mu)$. This angle must always be greater than zero -- in other words, the extinction angle β must be large enough to exceed the overlap angle μ at all load currents. If current overlap is included in the determination of the mean load voltage, then

$$E_{d.c.}' = E_{d.c.} \frac{\cos(\pi - \beta) + \cos(\pi - \beta + \mu)}{2} \quad (1.3.2)$$

by substituting $\alpha = (\pi - \beta)$. That the above then produces a negative voltage is shown by

$$E_{d.c.}' = -E_{d.c.} \frac{\cos \beta + \cos(\beta + \mu)}{2} \quad (1.3.3)$$

Inversion thus always drags lagging reactive power from the load.

1.4 Cycloconverter Application

As stated in the Introduction, the cycloconverter consists of two basic groups of rectifiers, often called the positive and negative groups. Each group consists of thyristors connected in this case so as to provide a full

wave circuit. The current to the load from each respective group can flow only in one direction. Therefore, since the a.c. output has an average value of zero, the two groups are connected back-to-back in the circuit. Simply alternating the firing of the two groups would result in an a.c. output of sorts. Rissik designated this type of operation "envelope cyclo-conversion"; it is merely a controlled rectifier in which the rectified current is alternated between positive and negative values.³ Because of the natural commutation, non-resistive loads are not permissible, since there can be no power regeneration back across the circuit. In order to obtain this power regeneration as well as voltage control, the firing angle must be phase controlled. This phase controlled cycloconverter can thus supply inductive loads by operating the rectifier group in the inverter mode. Since, at any instant, both rectifying groups and inversion groups are available to conduct the load current, loads of virtually any power factor may be controlled by the cycloconverter.

If the input circuit is polyphase, the output

becomes smoother, having lower harmonic content. In the case of a three phase full wave cycloconverter, the lowest harmonic frequency is six times the input frequency. The higher the frequency of the lowest harmonic, then the smaller the realizable filter can be, if needed. If the load is an a.c. synchronous motor, then the unfiltered output is sufficient to operate the machine, for the higher harmonics have no measurable effect on speed control.

It was demonstrated previously that the output of the rectifier group is $E_{d.c.}' = E_{d.c.} \cos \alpha$ in the rectifier mode of operation, and $E_{d.c.}' = -E_{d.c.} \cos \beta$ in the inversion mode. Thus the average output voltage may be varied between $E_{d.c.}$ and $-E_{d.c.}$. To achieve a sinusoidal variation in the output voltage, the firing angles α and β must be varied smoothly and sinusoidally at the desired output frequency ω_L . $0 \leq \alpha \leq \pi$ and $\pi \leq \beta \leq 2\pi$ and $\alpha, \beta = f(\omega_L t)$. The output of the cycloconverter is not a function of the low frequency reference and can be represented by a Fourier Series.

$$V = \sum_{n=1}^{\infty} E_{d.c.} a_n \cos n \omega_L t \quad (1.4.1)$$

To be valid, the output waveform must be analyzed over the period of the low frequency waveform, as opposed to the input waveform. The ideal situation occurs when both the input signal and the low frequency reference signal are sinusoidal at the point in the circuit where the firing angle is determined. In this case, the output voltage equals

$$V = E_{d.c.} \cos \omega_L t \quad (1.4.2)$$

The amplitude of the fundamental component of frequency, ω_L , is $E_{d.c.}$, while there are no higher frequency harmonics in the ideal case. In the actual cycloconverter circuit developed for this report, the low frequency reference signal is sinusoidal, but the input waveform has been transformed into a ramp function, which can be normalized as

$$f(\omega_s) = \frac{2}{\pi} \omega_s t \quad (1.4.3)$$

The output voltage then must be

$$V = E_{d.c.} \sin \left(\frac{k\pi}{2} \cos \omega_L t \right) \quad (1.4.4)$$

In determining the Fourier content of this output waveform,

$$a_n = (-1)^{(n-1)/2} 2 J_n \frac{\pi k}{2}, \quad n \text{ odd} \quad (1.4.5)$$

where J_n is the Bessel function of the first kind.⁶ Thus

$$V = 2 E_{d.c.} J_1 \left(\cos \omega_L t - \frac{J_3}{J_1} \cos 3 \omega_L t + \frac{J_5}{J_1} \cos 5 \omega_L t \dots \right) \quad (1.4.6)$$

In the case where the maximum variations of the low frequency sinusoidal function is equal to the range of the ramp function ($k = 1$),

$$V = 1.15 E_{d.c.} \left(\cos \omega_L t - 0.127 \cos 3 \omega_L t + 0.004 \cos 5 \omega_L t \dots \right) \quad (1.4.7)$$

There are, of course, harmonics due to the input ripple, but as expressed earlier, the lowest ripple frequency for a three phase full wave cycloconverter is $6 \omega_s$. If $\omega_s = 60$ Hz., and $\omega_L = 10$ Hz., then in the 10 Hz. output waveform, the lowest harmonic of ripple frequency is 360 Hz., which can easily be filtered if necessary.

Each half wave of the low frequency output, then, consists of different portions of both half waves (full wave operation) of the supply voltage. The overall effect is the assimilation of the low frequency wave. The firing angle is at a maximum at the beginning and at the end of

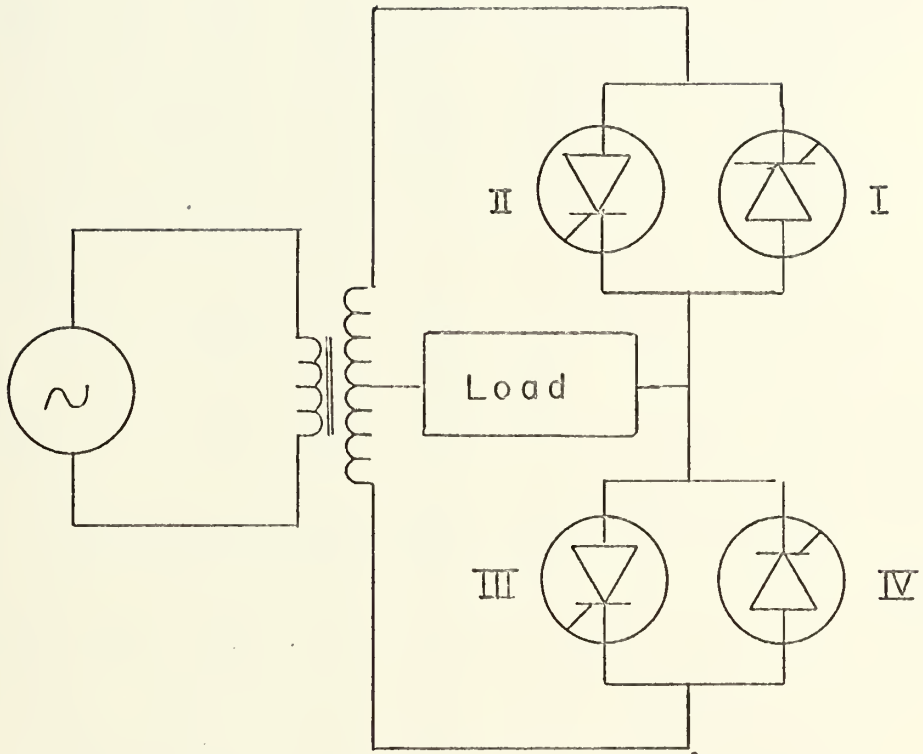
each half cycle of the output. At π , the firing angle is at a minimum. To produce the maximum value of output voltage, the firing angle must be equal to zero. The output voltage can then be subsequently reduced by limiting the minimum value of the firing angle α . To produce a zero output, the firing angle α is kept constant at $\alpha = \pi(1 - \frac{1}{n})$, where n is the number of phases. In the actual cycloconverter, α cannot equal 0, for in the inverter mode of operation, β (and consequently α , for symmetric operation) must exceed the delay angle μ .

In earlier cycloconverter configurations, firing pulses were given to both the positive and negative groups simultaneously. The result was intergroup circulating currents. These circulating currents were controlled by placing reactance in the intergroup circuit connections. A better solution was "blanking," or selectively firing one group of thyristors at a time, by detection of the polarity of the load current. The best solution of this problem is to selectively control the firing of each individual thyristor, for at any given

instant, only one thyristor in each output phase will be conducting. Thus digital logic is used to examine the state of the device and to select which thyristors are to receive the firing pulses.

There are three states which must be examined in order to determine the sequence of SCR firing. A simple full wave single phase to single phase cyclo-converter circuit is shown in figure 12. The decision of which SCR to fire is based on the polarity of the low frequency reference voltage, on the polarity of the load current, and on the polarity of the sinusoidal supply voltage. These logical states are designated LV, LI, and SV respectively. The polarity of a wave is considered here only to have two states: positive and negative. The zero-crossing is approximated to be instantaneous and is not given a state value.

A truth table (Table 1) then can be formulated in terms of the state variables.⁷ A logical 1 in the truth table corresponds to positive polarity of the state variable. A logical 1 in the output implies that



Single Phase to Single Phase
Cycloconverter

Figure 12

States		Outputs				
V	I	SV	I	II	III	IV
0	0	0	0	1	0	0
0	0	1	0	0	0	1
0	1	0	1	0	0	0
0	1	1	0	0	1	0
1	0	0	0	0	0	1
1	0	1	0	1	0	0
1	1	0	0	0	1	0
1	1	1	1	0	0	0

Truth Table
Table I

a firing pulse is to be applied to the indicated SCR -- it says nothing yet about the nature of this firing pulse. Karnaugh maps⁷ are then derived for each output function, in order to get minimal logical expressions (Table 2). Unfortunately, the Karnaugh maps demonstrated that the expressions for each of the logical functions could not be minimized beyond the canonic forms (Standard Sum of Products). The resulting switching functions for each output are

$$I = LV \cdot LI \cdot SV + \overline{LV} \cdot LI \cdot \overline{SV} \quad (1.4.8a)$$

$$II = LV \cdot \overline{LI} \cdot SV + \overline{LV} \cdot \overline{LI} \cdot \overline{SV} \quad (1.4.8b)$$

$$III = LV \cdot LI \cdot \overline{SV} + \overline{LV} \cdot LI \cdot SV \quad (1.4.8c)$$

$$IV = LV \cdot \overline{LI} \cdot \overline{SV} + \overline{LV} \cdot \overline{LI} \cdot SV \quad (1.4.8d)$$

When $LV = LI$, the cycloconverter is operating in the rectification mode, and power is being delivered to the load. When $LV \neq LI$, the cycloconverter is operating in the inversion mode, and power is being regenerated back to the source supply. Now positive blanking is achieved, and intergroup currents are prevented. The functions are in terms of minimal sum of products expressions and can be easily realized using

		V, I			
		00	01	11	10
SV	0	0	1	0	0
	1	0	0	1	0

I

		V, I			
		00	01	11	10
SV	0	1	0	0	0
	1	0	0	0	1

II

		V, I			
		00	01	11	10
SV	0	0	1	0	0
	1	0	1	0	0

III

		V, I			
		00	01	11	10
SV	0	0	0	1	0
	1	1	0	0	0

IV

Karnaugh Maps

Table 2

conventional logic circuitry.

It was stated earlier that the a.c. input supply voltage was converted to a ramp function having the same period as the supply voltage. In actuality, two ramps are generated; one ramp has a period from $-\pi$ to π , while the second ramp has a period from 0 to 2π . The low frequency reference signal is then superimposed on both ramps to determine the firing angle for the thyristors. As the low frequency signal increases from zero, the firing angle α decreases from π towards zero on the ramp having the period from 0 (or 2π) on the other ramp. If the low frequency signal in turn is inverted and superimposed upon the ramps, the firing angle α will be increasing from π and 0 respectively. Thus, there are four simultaneous variations of the firing angle depending upon which circuit is selected: for the low frequency sine wave increasing from zero, these are the firing angle α decreasing from π ($\pi \downarrow$), decreasing from 0 ($0 \downarrow$), increasing from π ($\pi \uparrow$), and increasing from 0 ($0 \uparrow$). The truth table can now be amended as in Table 3. In the next chapter, it will be

States			Outputs			
V	I	SV	I	II	III	IV
0	0	0	-	0↓	-	-
0	0	1	-	-	-	π ↑
0	1	0	π ↑	-	-	-
0	1	1	-	-	0↑	-
1	0	0	-	-	-	π ↑
1	0	1	-	0↑	-	-
1	1	0	-	-	0↑	-
1	1	1	π ↓	-	-	-

Modified Truth Table

Table 3

shown that these conditions can be combined with the logical expressions developed earlier to generate the proper firing angle for each thyristor.

1.5 Three Phase Low Frequency Generation

In most cycloconverter applications, any variable frequency three phase reference voltage is sufficient for proper operation of the device. If three phase cycloconverter operation is desired, then the only requirement upon the variable frequency oscillator is that it be three phase with constant phase relationship throughout the frequency range of the oscillator. A very easy way to do this is by using two multipliers and two integrators. This produces a two phase oscillator, whose phases are always ninety degrees apart. From these, three phasors, 120 degrees apart in phase, can be produced, yielding a three phase voltage controlled sine wave generator.

In order to drive a synchronous motor mounted directly on the propellor shaft, it is desirable to feed back the information regarding not only the shaft speed, but also the relative position of the rotor with respect to the rotating flux wave produced by the current in the armature. The torque produced by the motor onto the

shaft is a function of the air gap flux Φ_a , the rotor mmf F_r and the torque angle γ_r representing the lag of the rotor mmf wave with respect to the air gap flux wave.⁸ One expression for the torque in a synchronous machine is

$$T = \frac{\pi}{2} \left(\frac{\text{poles}}{2} \right)^2 \Phi_a F_r \sin \gamma_r \quad (1.5.1)$$

The rotor mmf F_r is determined by the exciter current in the field, and is constant under normal operation.

$$F_r = \frac{4}{\pi} k_r \frac{N_r}{p} I_r \quad (1.5.2)$$

k_r = winding factor

N_r = number of turns on the rotor

p = number of poles in the machine

The air gap flux Φ_a is a function of many constants and the instantaneous value of the armature current.

$$\Phi_a = \frac{8}{\pi} k_s \frac{N_s}{2} \frac{d l \mu_o}{g} I_a \quad (1.5.3)$$

k_s = stator winding factor

N_s = number of turns in the stator

d, l, g = dimensions of the machine

μ_o = permeability of the iron circuit

I_a is the fundamental a.c. armature current being supplied

by the cycloconverter. Thus the torque available to the load can be varied by varying the armature current produced by the cycloconverter, if the torque angle is held constant. Maximum torque for the machine at rated current occurs when the torque angle $\gamma_r = \pi/2$. Therefore, if it is desired to maintain γ_r at approximately $\pi/2$, then the rotor position (which implies the spatial position of the rotor mmf) must be sensed, such that the reference voltage of any phase can lead the rotor flux by the required amount to produce maximum torque.

The best way to indicate the shaft position is to mount a Selsyn generator, or other appropriate electro-mechanical transducer, directly on the shaft. The Selsyn generator has a single phase winding on the rotor connected to an a.c. voltage source. The stator has three windings with axes 120 degrees apart and connected in wye. When the single phase rotor winding is excited, voltages are induced by transformer action in the stator windings. The resultant waveform is the impressed a.c. frequency modulated by the mechanical frequency of the shaft. In addition, the absolute position of the shaft with respect

to any winding is indicated by the amplitude of the carrier signal on the winding at that instant. The signal from each of the three stator windings must be demodulated, as well as phase detected. This can be done by a two diode shunt demodulator as shown in the next chapter. The resultant low frequency sine waves are 120 degrees out of phase with each other, and have a direct correspondence to actual shaft position. Thus the maximum torque angle can be controlled. Then to increase shaft speed, only the amplitude of the current through the cycloconverter must be increased, as explained above. The phase relationship can be reversed to reverse the motor, thus providing the required full range of operation.

Chapter II

Design Applications and Circuits

2.1 Cycloconverter Section

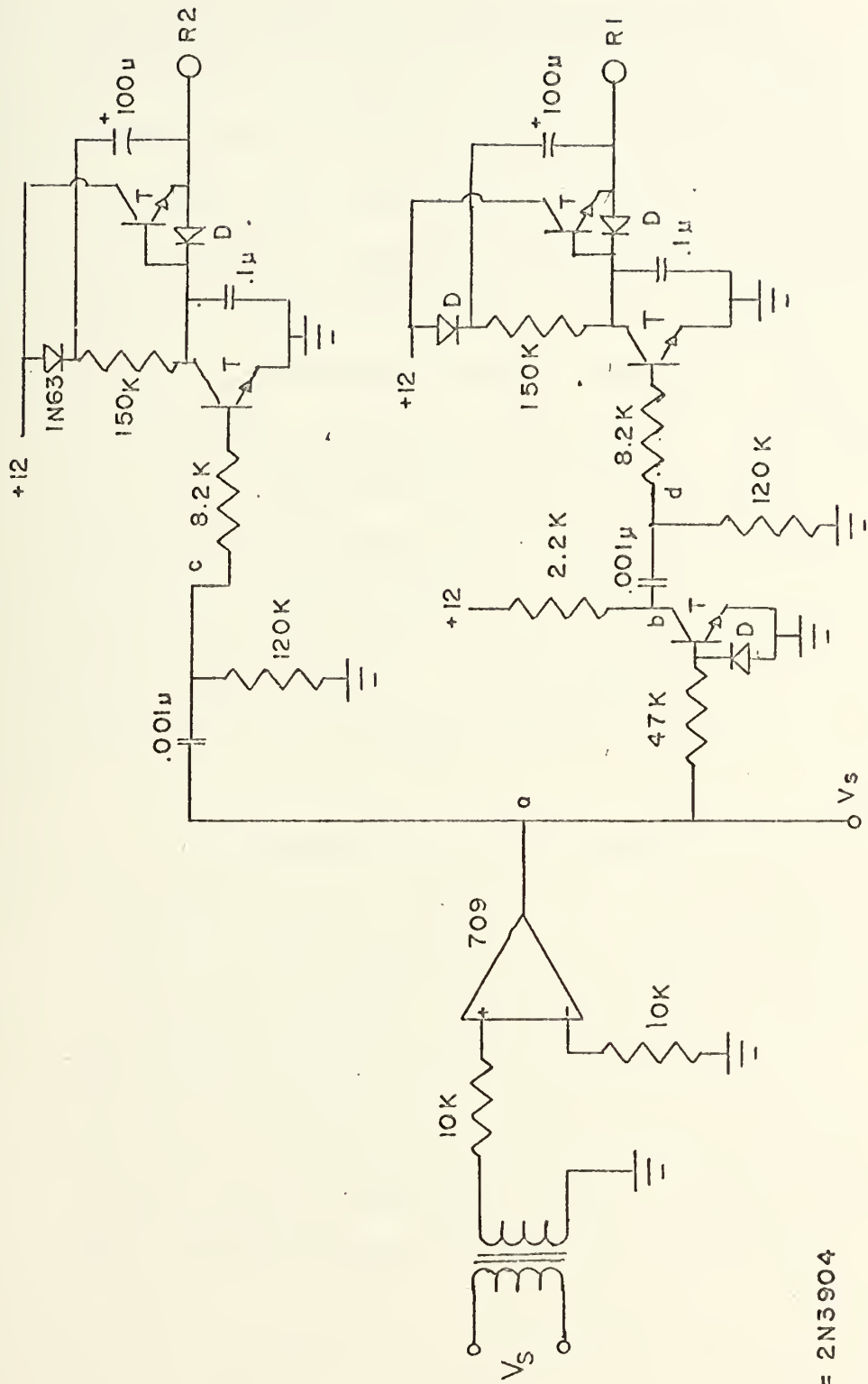
The cycloconverter consists basically of two major units, each of which will be considered separately. The thyristor section can also be designated the power section, for it consists mainly of the power thyristors themselves plus the load and protective circuitry. The other major unit is the triggering network. This low power level section generates the firing signals that are applied to the gate of each thyristor.

2.1.1 Triggering Network

There are three basic inputs required by the triggering network. These are the input supply voltage, the low frequency reference voltage and the load current signal. The output of the triggering network is a firing signal to each SCR, properly phase controlled and of sufficient power to fire the SCR reliably. The

triggering network discussed below is then the heart of the cycloconverter, and critical to its operation. The particular network discussed is only for one phase input to one phase output operation. To produce three phase input to three phase output operation, nine identical modules can be used, each connected to a different combination of input and output phases. The triggering network can be divided into four sections: the ramp generators, the summing circuit, the digital logic, and the trigger circuits.

The ramp generator section is shown in figure 13. The transformer steps the supply voltage down to an acceptable level so as not to exceed the differential input voltage of the operational amplifier. The operational amplifier, having a very high input impedance, requires no more than a potential transformer to provide the reference voltage. The operational amplifier acts as a comparator or sign detector. The waveform at point a is then a square wave varying between +12 and -12 d.c. volts, having the same frequency as the input supply. The waveform then goes into two circuits at this point.



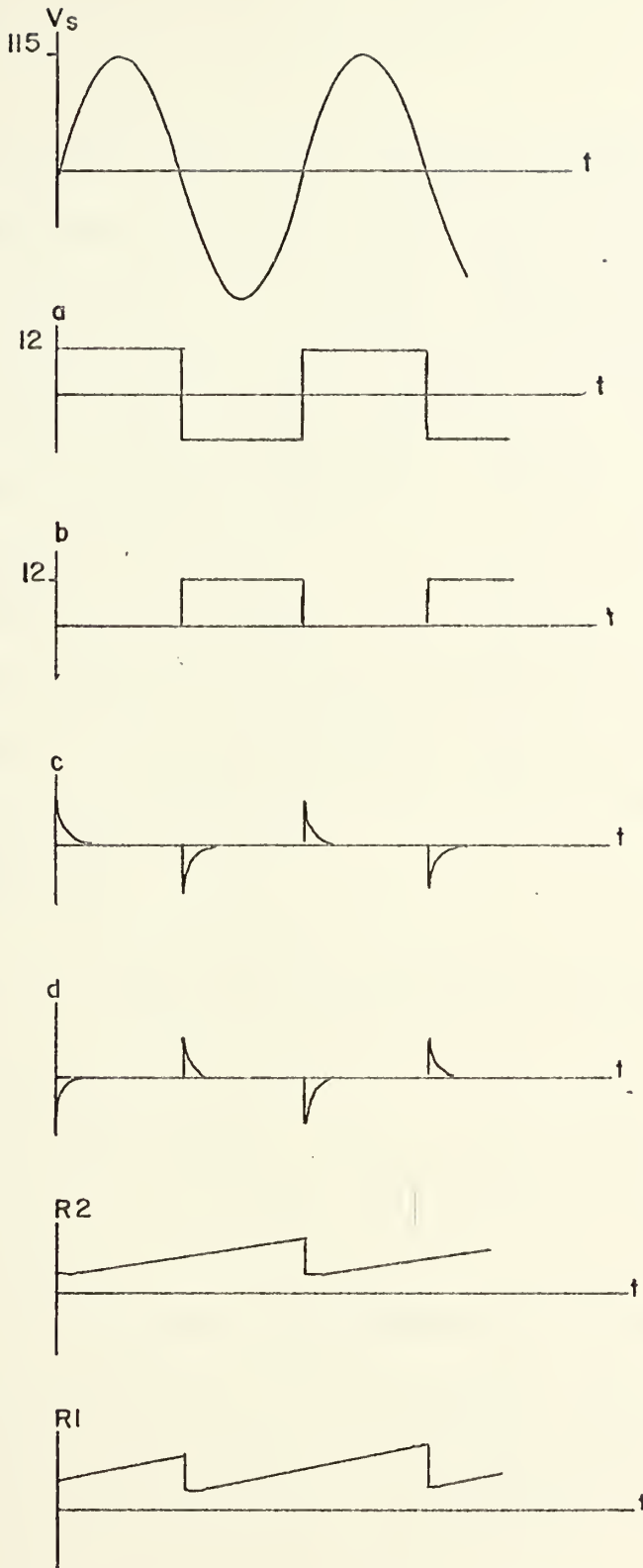
T = 2N3904

D = IN63

Ramp Circuit
Figure 13

One circuit consists of a pulse generator (an RC differentiator) which drives a linear sweep circuit having a period of 2π (initiated by a positive pulse, and resetting at each succeeding positive pulse). The linear rise is caused by a constant current charging the 100 μf capacitor. The waveform at point a also is inputted into the base of a transistor inverter. Thus, at point b, the waveform is the inverse of that at point a, or delayed by $\omega t = \pi$. This inverted waveform goes through an identical pulse generator and linear sweep circuit, producing a ramp, R2, which is 180 degrees out of phase with the first ramp, R1. The waveforms are shown in figure 14, for the labelled points in the circuit.

The second unit in the triggering circuit is the summing circuit. In this section the low frequency reference signal is added to the ramp functions generated in the previous section. The ramp generators require a high impedance load, provided by the 100 K impedance levels of the adder circuit. The operational amplifiers are again used as comparators, with the comparison levels being adjustable voltages in order to set the initial

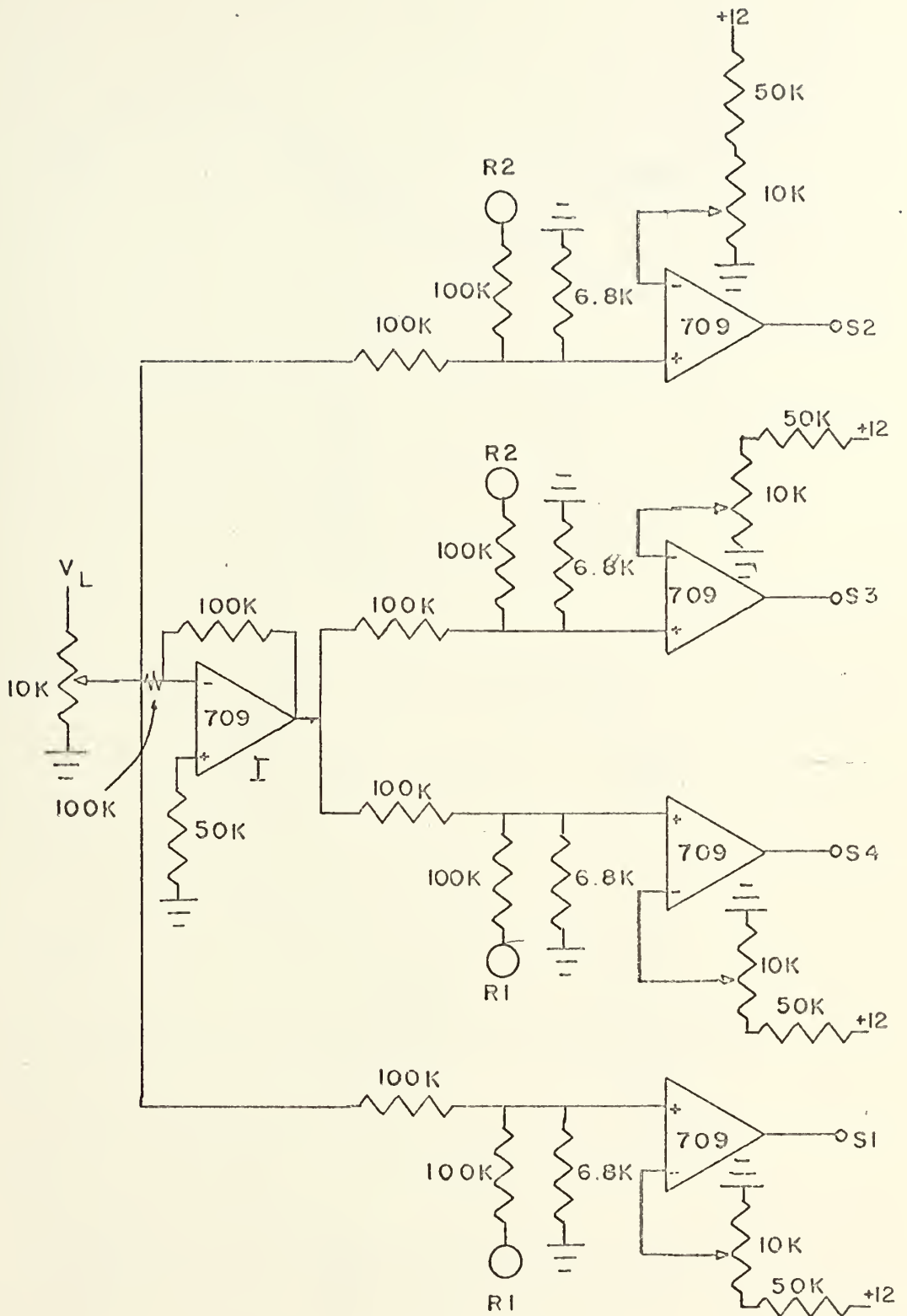


Voltage Waveforms in Ramp Circuit

Figure 14

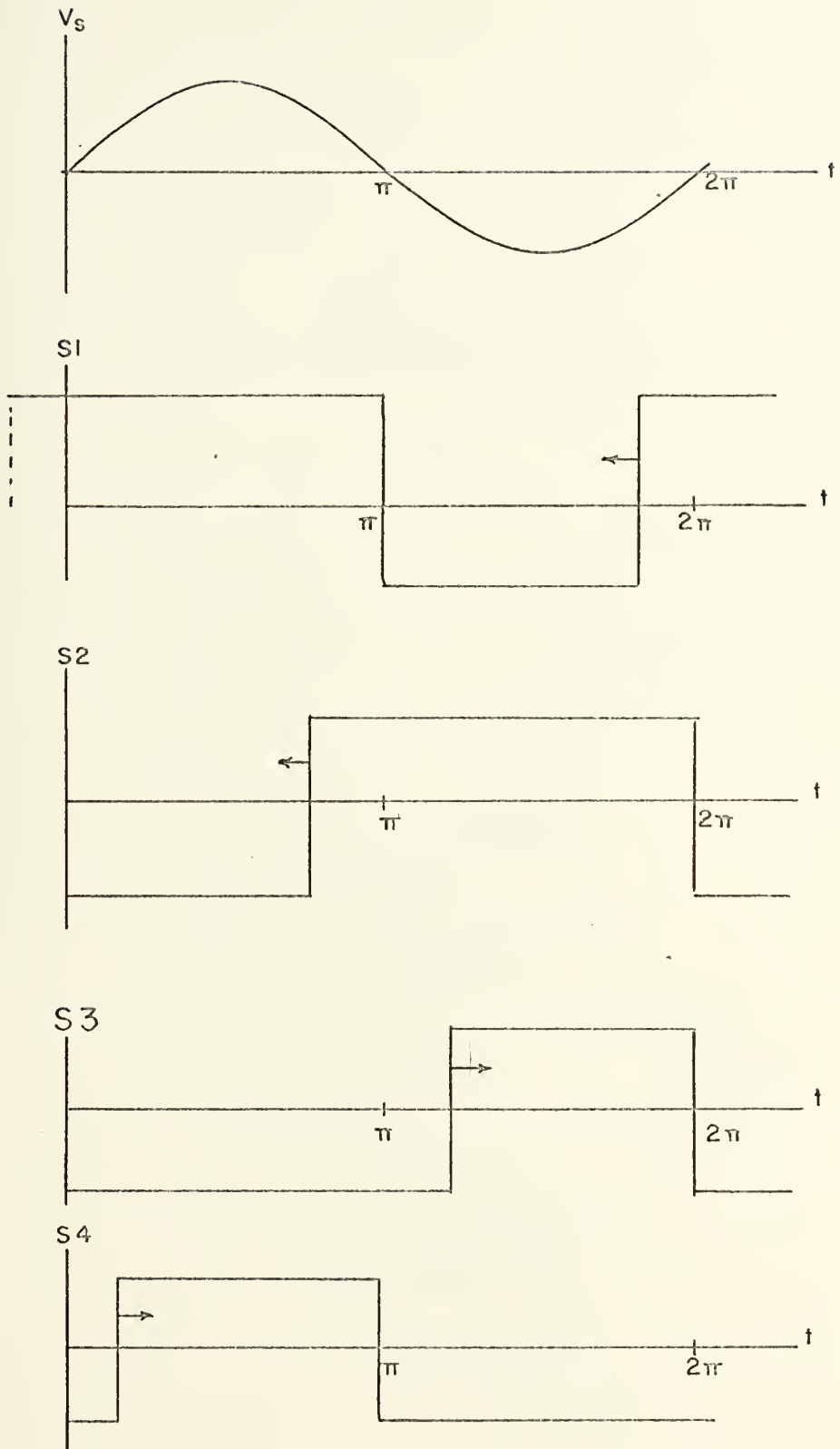
firing point, when the low frequency voltage is deenergized, at a point on the ramp corresponding to the exact middle of the period. The low frequency voltage then moves the firing point up and down the ramp -- the range being adjusted by adjusting the output voltage of the low frequency generator. Figure 15 is a circuit diagram of the adder section. The operational amplifier labeled I is an inverter having a gain of -1. It is used to invert the low frequency function, in order to sweep the ramp in the opposite direction. The output waveforms, corresponding to $V_L = \pi/4$, are shown in figure 16.

The third section of the firing circuit is the digital logic section. This section is subdivided into two further sections. The first subsection, shown in figure 17, realizes the truth table given in Table 1 of Chapter 1. DTL (Diode-Transistor-logic) components are used to facilitate the interface with the rest of the analog circuitry, and additionally to drive the required number of gates (RTL has difficulty driving more than 3 gates without the use of a power gate). The transistor

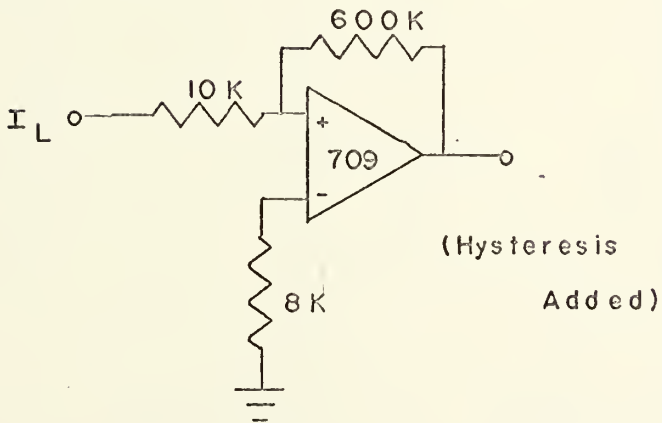
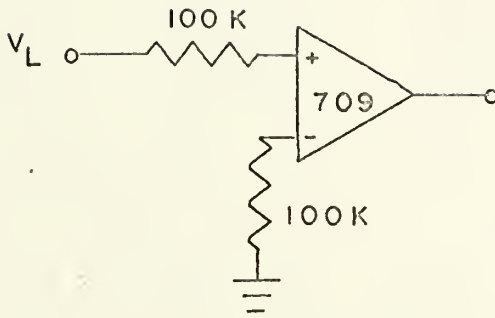


Summing Circuit

Figure 15

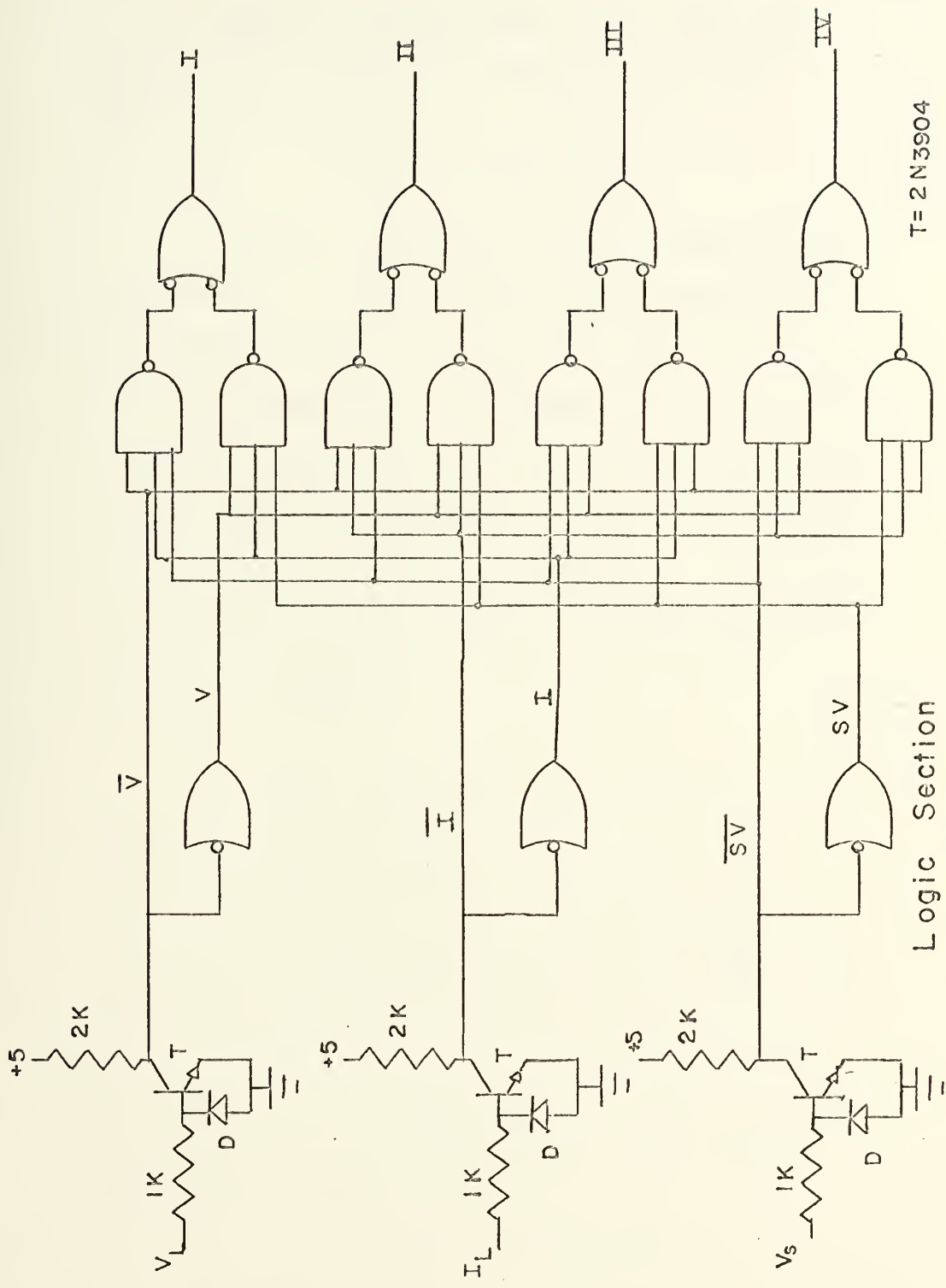


Waveforms of Summing Circuit
Figure 16



Sign Detectors

Figure 17a



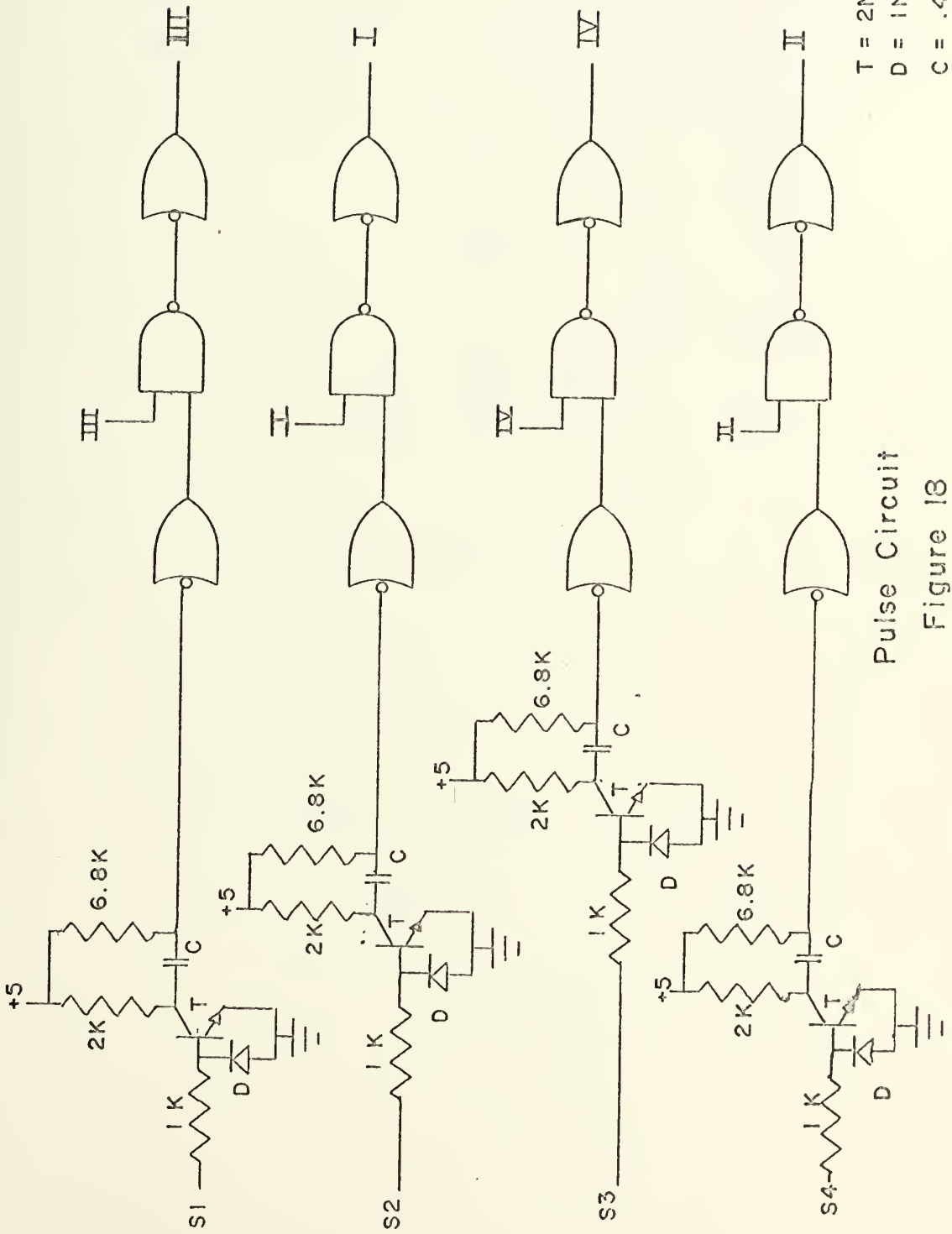
T = 2N3904
D = 1N63

Logic Section
Figure 17b

circuits change the voltage levels of the operational amplifiers from +12 and -12 volts to +5 and 0 volts required by the digital logic.

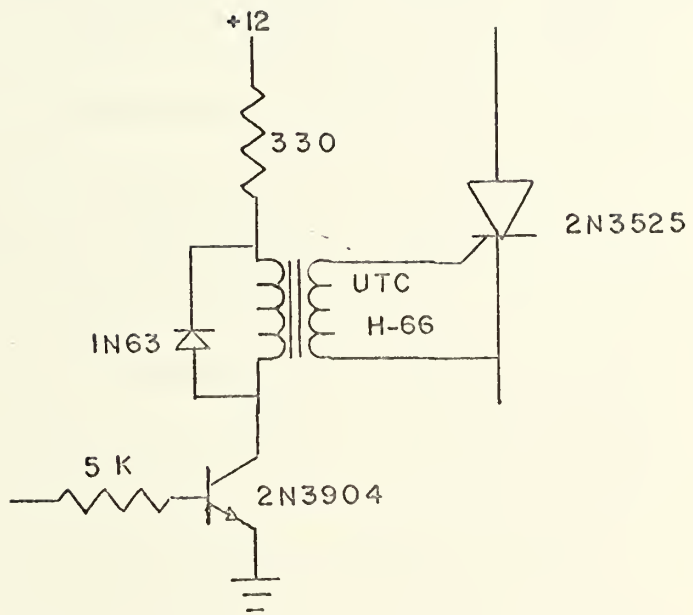
The second subsection, shown in figure 18, has two functions. It employs monostable multivibrators (or pulse generators) which are triggered on the rising edge of the pulses generated in the summing circuit. The output of these pulse generators are 1 millisecond pulses, which are then "anded" with the outputs of the first subsection to realize finally the Table 3 of Chapter 1. The result is that firing pulses are available to be applied to the gates of the SCR's.

The SCR's are connected anti-parallel, but the trigger must always be applied from the gate to the cathode. Therefore, the actual firing circuits must be isolated from the individual thyristors. The pulse transformers provide the required isolation, and in conjunction with the accompanying transistor circuit (figure 19), provide the level of gating current to insure reliable operation of the SCR's.



T = 2N3904
 D = 1N63
 C = .47μF

Pulse Circuit
 Figure 18



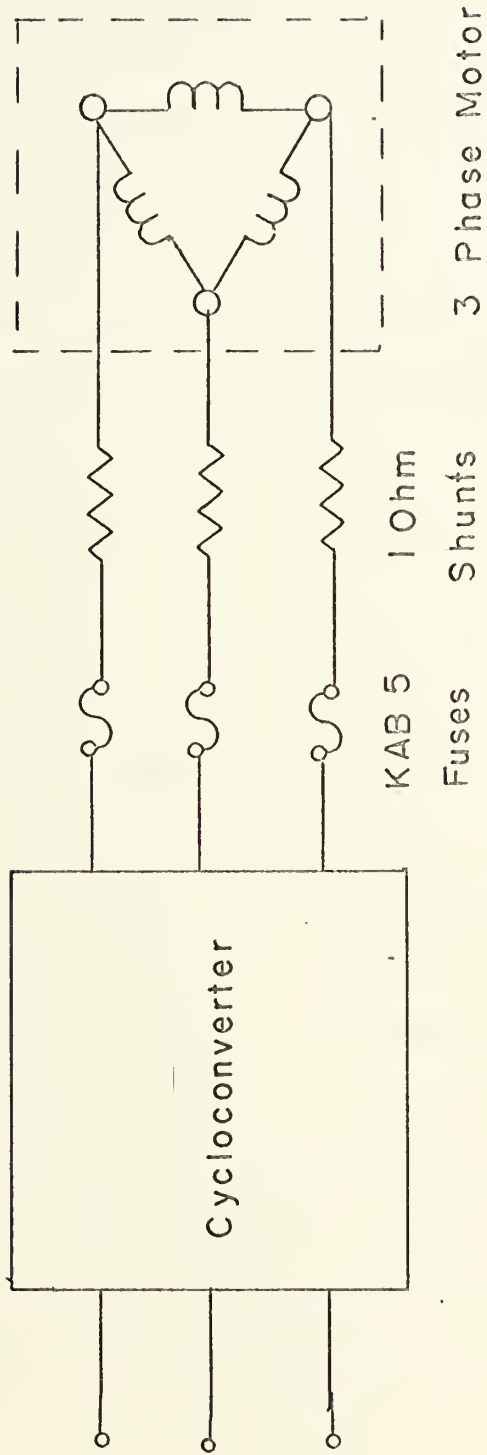
Trigger Circuit

Figure 19

2.1.2 Thyristor Network

The thyristors are connected as shown originally in figure 1. Full rated fuses are inserted in each of the input voltage supply networks. The motor is then placed directly in the output of the cycloconverter. The only additional circuitry is the insertion of phase current detectors (figure 20). Shunts are used to provide the current polarity reference signal to an operational amplifier with sufficient hysteresis in the feedback to eliminate spurious noise and high frequency harmonics about the zero cross-over. These current shunts are placed in the low voltage side of the motor, and can be interfaced directly with the trigger circuitry. The shunt must be rated so as to provide no more than 5 volts voltage drop for the maximum current rating of the motor, in order not to exceed the differential input voltage limitation of the operational amplifier.

To convert three phase, 60 hertz power to three phase, variable frequency power requires a minimum



Motor Drive Circuit

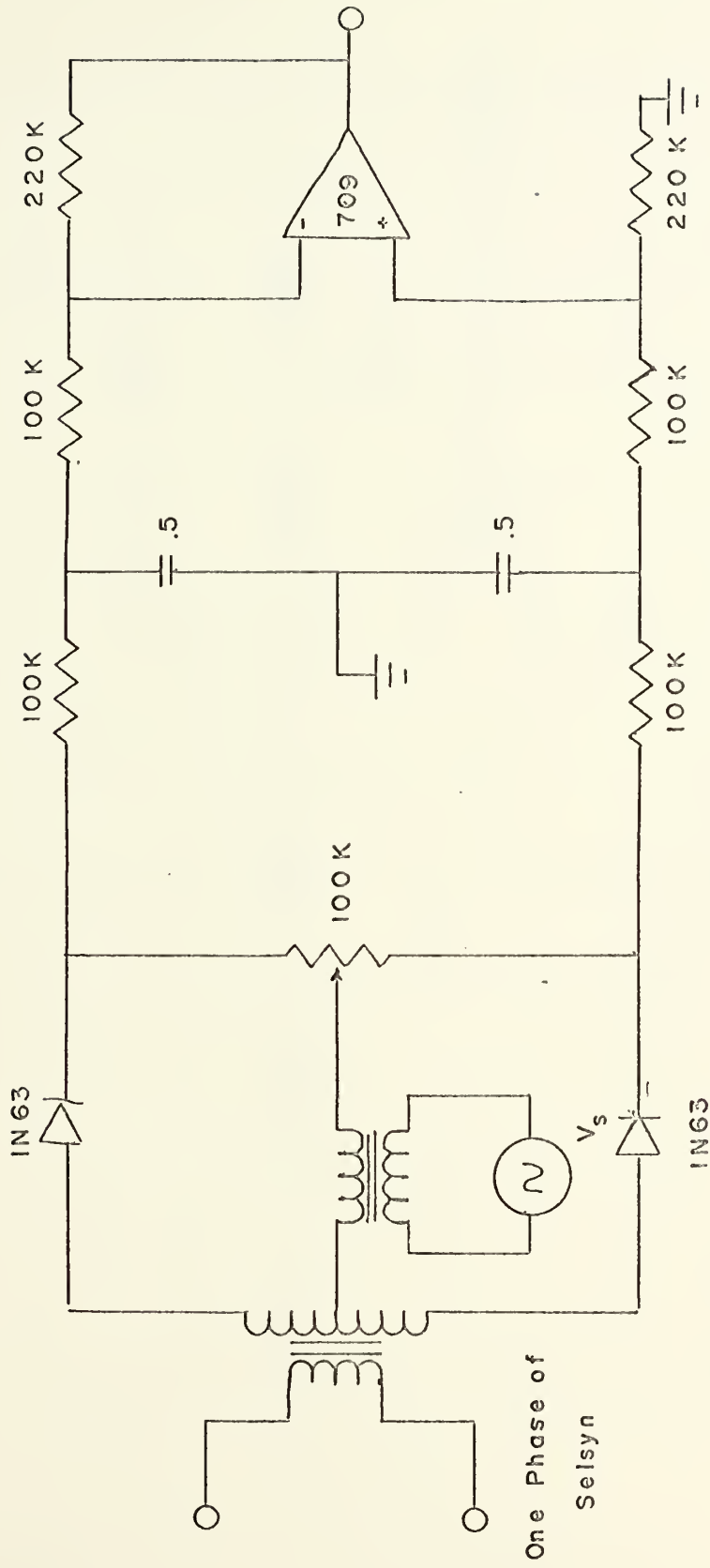
Figure 20

of 36 thyristors (3 circuits identical to figure 1). The capability of each SCR is based upon the peak voltage which it must block in either direction, as well as the RMS current it must conduct under complete conduction conditions. The system proposed in reference 1 requires each phase to conduct 615 amperes maximum, and block 3850 peak volts. To provide for reliable operation, SCR's that are currently available which are able to handle this amount of current must be operated in series of at least three to reduce the voltage blocking requirements. When operated in series, additional voltage equalizing networks must be employed to prevent overloading any one SCR. These SCR assemblies will have to be water cooled with at least one gpm. for each set of three SCR's to dissipate the thermal energy produced at the junction. No external cooling is needed for the control circuitry, however. If voltage regulated power supplies are constructed for providing the necessary +12, -12 and +5 d.c. voltage levels needed in the control unit, the power requirement is so small that individual power transistors in the power supplies can be cooled convectively simply by attaching small heat sinks.

2.2 Low Frequency Reference Generation

It was stated in Chapter 1 that a demodulation circuit is required to generate the variable frequency reference voltage supplied to the triggering network. Not only are variable frequency, constant phase separated, three phase reference voltages required, but also the signal must be directly phase associated with the position of the rotor in the synchronous motor in order to optimize the torque angle.

A three winding Selsyn generator is directly coupled to the shaft of the synchronous motor. The rotor of the Selsyn generator receives a high frequency voltage available from the high frequency side of the cycloconverter through slip rings. The three stator windings are connected to three transformers with the secondary center-tapped. A demodulator (see figure 21) is used to provide the required reference frequency, dependent upon the speed of rotation as well as the actual phase position of the rotor. The demodulator is the two diode shunt demodulator⁹ and acts as a phase detector as well as a



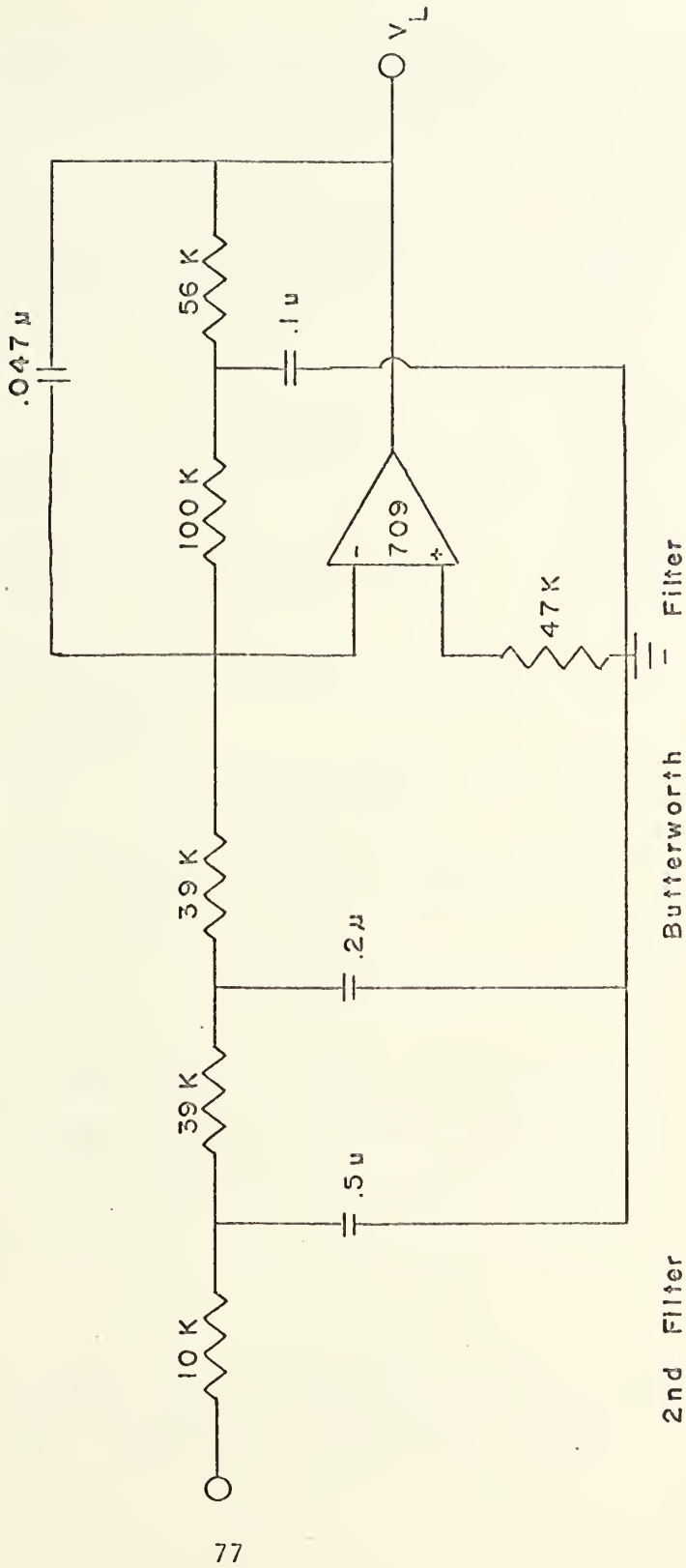
Differential Amplifier

First Filter

Demodulator

Demodulator Circuit

Figure 21a



Filter Circuit
Figure 21b

demodulator. The voltage out of the Selsyn generator is described as

$$V = V_m \cos \omega_L t \cos \omega_s t \quad (2.2.1)$$

The reference voltage is added and subtracted to this signal

$$V_r = V_{rm} \cos \omega_s t \quad (2.2.2)$$

The addition of the reference voltage produces

$$V_1 = \frac{V_m \cos \omega_L t + V_{rm}}{\pi} \quad (2.2.3)$$

While the subtraction of the reference voltage simultaneously produces

$$V_2 = \frac{-V_m \cos \omega_L t + V_{rm}}{\pi} \quad (2.2.4)$$

The output of each demodulator circuit then becomes

$$V_1 - V_2 = V_L = \frac{2 V_M \cos \omega_L t}{\pi} \quad (2.2.5)$$

and separated in phase from each other by 120 degrees. Even when the propellor shaft is at dead stop, there is a phase voltage on each phase indicating the angular position of the shaft.

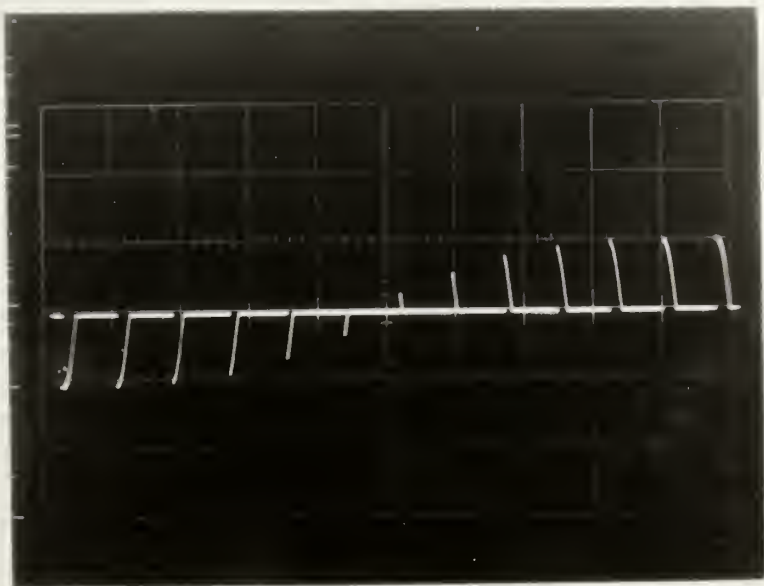
The signal from the demodulator must be filtered and sent through a differential amplifier in order to

transform the balanced waveform into a voltage about the circuit ground. A single feedback, high pass Butterworth active RC filter is used to smooth the waveform to the level required by the triggering circuit. The output of this filter is then sent directly to the summing section of the triggering network, as described previously. The Butterworth filter was designed for a maximally flat response with a 40 db/decade rolloff.

Chapter III

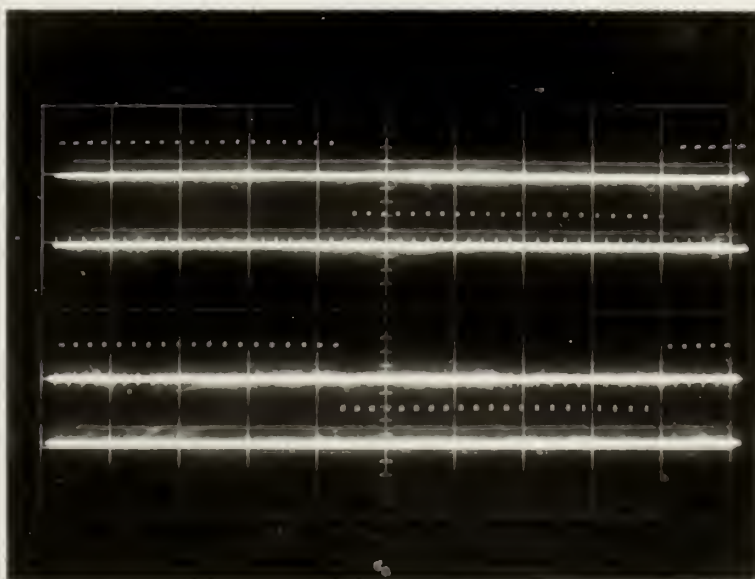
Analysis of Performance

In order to test the cycloconverter circuit under various load conditions with a wide range of load power factors, several devices were inserted into the cycloconverter load circuit. A wire-wound resistance of 108 ohms was inserted first as the load. The frequency was controlled by a separate function generator. The frequency range was varied over a complete range from 0 hertz to 30 hertz (the supply frequency to the cycloconverter in all cases is 60 hertz). The voltage across the load was displayed on an oscilloscope. Figure 22 is a photograph of the load voltage waveform, clearly showing the sinusoidal variation in firing angle. All of the oscilloscope settings for each photograph are given in Appendix B. There was only a slight inductance in the circuit, caused by the inductance of the wire-wound load resistor. The current waveform was then essentially identical to that of the voltage, and in phase with the voltage. With a resistive load, there is no inversion mode in the cycloconverter, and only the thyristors



Resistive Load Voltage

Figure 22



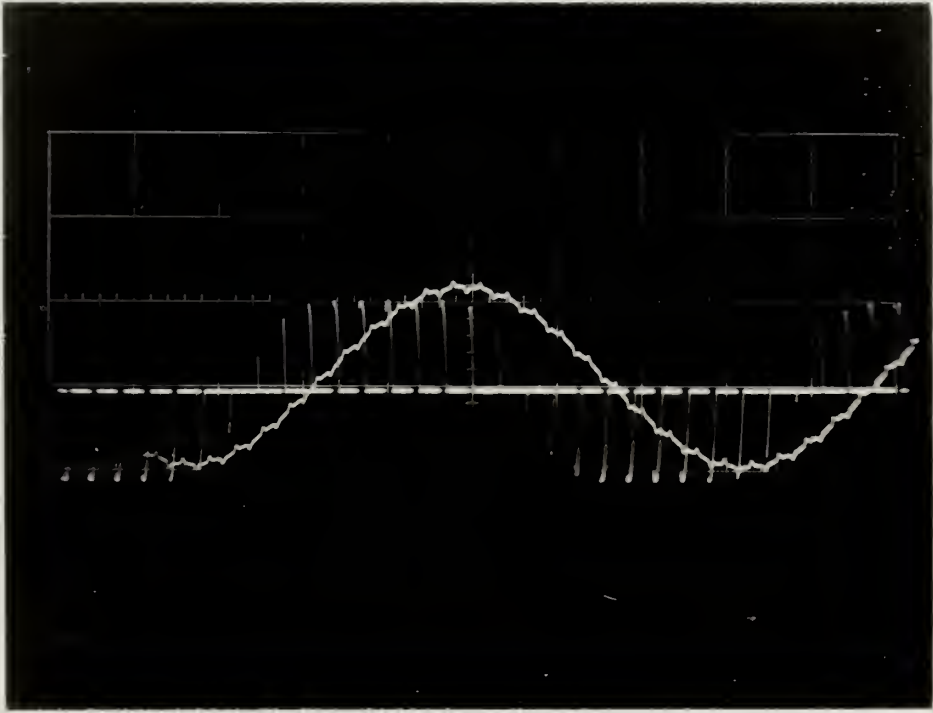
Firing Pulses

Figure 23

labeled I and II in figure 12 will receive firing pulses, during the positive half cycle of the low frequency voltage, while only thyristors II and IV will receive firing pulses during the negative half cycle. This is shown in figure 23. The top trace on the oscilloscope is the firing pulse train to thyristor I, the second trace is the firing pulse train to thyristor II, and so forth.

Inductance was then added into the load circuit, and the resistance was reduced to 25 ohms. The total impedance of the load then became $Z = 27.2 + j24.5$ ohms, at a frequency of 6 hertz. This inductance was sufficient to smooth the current waveform, in order that it could be graphically displayed in figure 24. The smoothed waveform is the current waveform, which is shown to lag the voltage waveform by approximately 42 degrees, which agrees with the calculated lag.

The first motor employed in the load circuit was a one quarter horsepower, permanent-split-capacitor synchronous motor (single phase). The motor was loaded



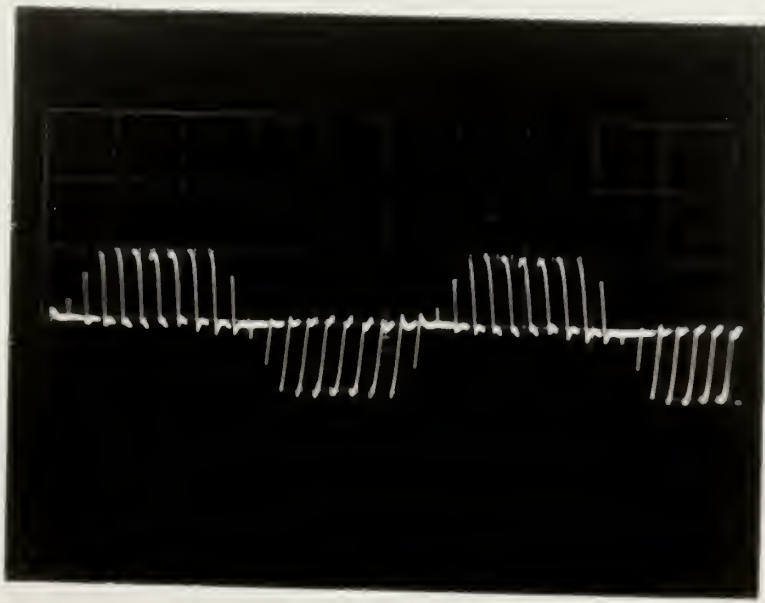
Continuous Waveform is
Load Current

Voltage and Current in Inductive Load

Figure 24

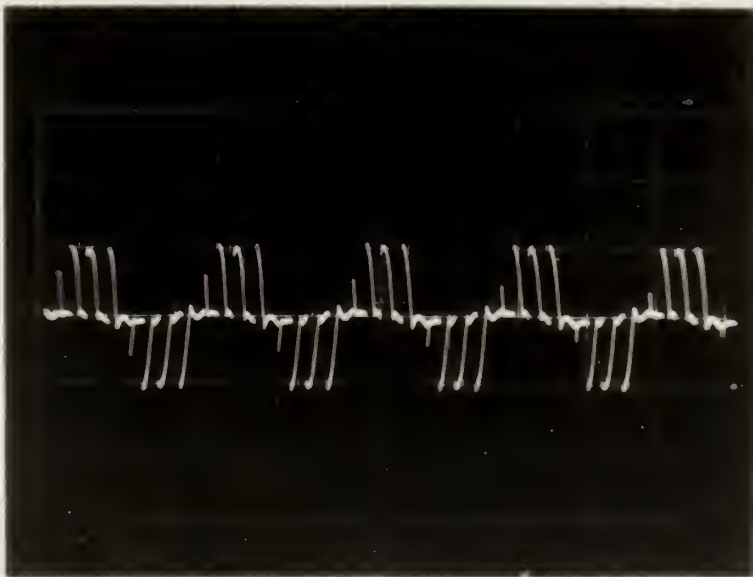
only by its own shaft friction. The starting characteristics of the motor were poor when low frequency (less than 10 hertz) power was applied to the stators, because the permanent capacitance in the split phase circuit was a tradeoff between efficient starting at 60 hz. and smooth continuous operation at rated speed. The motor has difficulty in generating sufficient torque to operate at a frequency below approximately 5 hertz. Again the frequency was controlled by a variable frequency function generator. The shaft speed was measured by a Strobotac, triggered by the frequency generator. The motor was then observed to operate in precise synchronism with the reference low frequency voltage from the function generator. The voltage waveforms for the machine operating at 180 RPM (6 hz.) and 450 RPM (15 hz.) are shown in figures 25a and b respectively.

Finally a single-phase, shaded pole one quarter horsepower synchronous motor was connected to the single phase cycloconverter. At a prescribed low frequency output of the function generator, the motor came up to



Motor at 180 RPM

Figure 25a



Motor at 450 RPM

Figure 25b

speed as an induction motor and snapped into synchronism. At this time, mechanical shaft load would be applied to the shaft manually, and the motor would remain synchronous while the torque angle would increase. The frequency generator system was then connected to the synchronous motor in order to test the proposed control system. The Selsyn generator was connected to the shaft of the synchronous motor by a flexible shaft coupling in order to insure that the Selsyn generator would be driven at the same speed as the synchronous motor. The position of the Selsyn with respect to the spatial position of the rotor of the synchronous motor was adjusted so that the output of the frequency generator was in phase with the low frequency voltage applied to the motor. The motor would not self start, because of the inherent limitations of the single phase motor. This problem will not be encountered with a full scale system employing synchronous motors with three phase stator windings.

Synchronous motors can operate very well on an extremely rough waveform. It is generally accepted that the waveform of a cycloconverter operating above

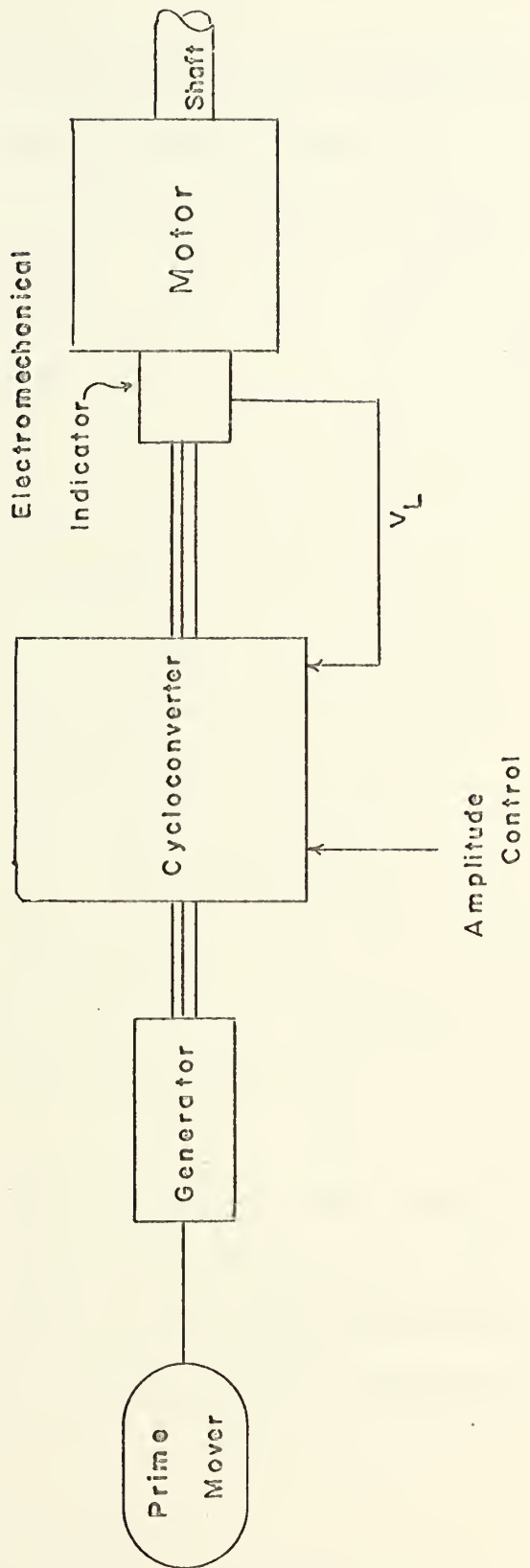
approximately one third of the input frequency is unusable. It was demonstrated, however, that a synchronous motor controlled by a full wave cycloconverter could be operated at the predicted synchronous speed up to even one half of the input frequency. Even though the voltage waveform was quite rough, the fundamental frequency dominated sufficiently to drive the rotor in synchronism.

Chapter IV

Conclusions

The results of the operational tests described in the previous chapter that were applied to the single phase to single phase cycloconverter indicate that the cycloconverter circuit designed above is a highly flexible synchronous motor controller. The cycloconverter control system (figure 26) has several distinct advantages over other motor control systems.

First, the machine can not be pulled out of synchronism by torque surges. Under normal synchronous motor drive systems, momentary surges of load torque beyond the value of pull-out torque will cause the rotor to pull out of step with the rotating flux wave in the stator. This loss of synchronism is not possible in the proposed propulsion system, because its speed control (or frequency control, since the speed of a synchronous motor is determined by the frequency of the armature voltage) is directly coupled to the propulsion shaft. If the rotor begins to slip out of synchronism, the three phase frequency generator drive in turn slows and sends a



Cycloconverter Control System

Figure 26

lower frequency reference signal to the cycloconverter. The cycloconverter then continuously lowers the frequency of the stator current, keeping its field in synchronism with the rotor. The motor could then be returned to the desired operating speed by adjusting the amplitude control on the cycloconverter. Increasing the amplitude of the stator current causes increased torque to be applied by the motor to the shaft. The shaft (and the rotor) will accelerate, and the frequency generator, attached to the shaft, will accelerate as well. Thus, as the shaft speeds up, the frequency of the current applied to the stator simultaneously increases, and the rotor remains in synchronism with the flux wave on the stator. When the desired operating speed is attained, the amplitude control on the cycloconverter is decreased until the applied torque of the motor equals the torque requirement of the load.

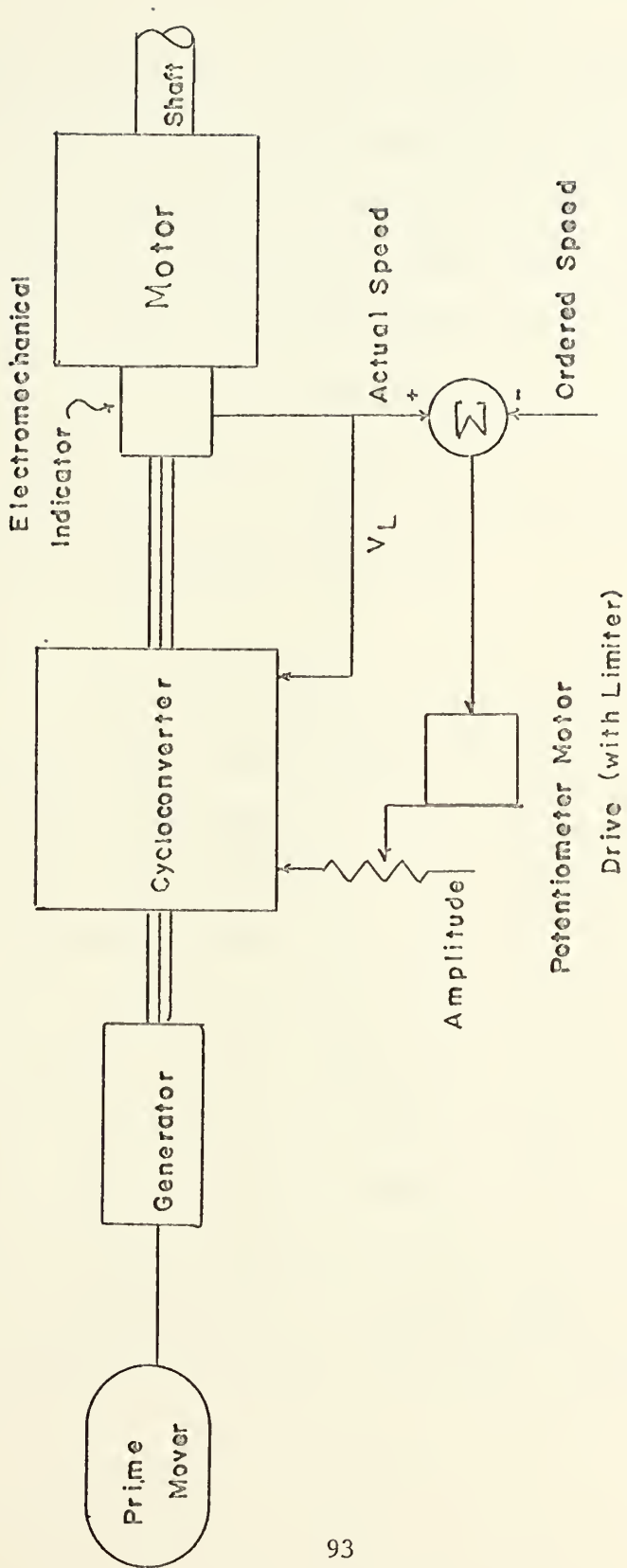
It can then be seen that a second significant advantage of the cycloconverter drive system is that the synchronous motor accelerates to the desired operating speed synchronously, even when the shaft originally is at

a stop. In normal synchronous motor systems, the synchronous motors come up to speed asynchronously by acting as induction motors. This occurs when voltage of the desired operating frequency is applied to the stator. When the rotor reaches synchronous speed, the rotor pulls into synchronism with the armature flux wave. The shaft torque produced by the machine when accelerating to operating speed asynchronously is not a function of the load torque, but is determined by the parameters of the motor. The cycloconverter control system of operation does not face these problems. The rotor is always in synchronism with the stator field, as explained above. The only starting torque required by the motor is the torque necessary to overcome the load torque, plus sufficient torque to accelerate the load at the desired rate. Synchronous starting of the motor is then quite smooth, and completely controllable at all times. Thus the acceleration can be controlled exactly by controlling the amplitude of the armature current.

The propulsion shaft, in addition, can be reversed by reversing the phase relationship of the

three phase reference frequency. The shaft then can be positively slowed by reversing the direction of torque applied in order to give a controlled deceleration.

The cycloconverter control system is a potentially attractive method of controlling synchronous motor propulsion systems, exhibiting fast response and positive control. In order to incorporate the above control system into a naval propulsion system, a speed control system must be incorporated into the overall design (figure 27). This controller will compare the actual speed of the propulsion shaft to the desired speed requested from the bridge and sends a feedback signal to a motor driven potentiometer, which controls the amplitude of the output current from the cycloconverter. The potentiometer can increase the amplitude of the current to accelerate the rotor if the shaft is operating under the desired speed, or it can decrease the current amplitude if operating overspeed. The speed controller must also have a limiter, which limits the rate of change of the potentiometer. The limit is a function of the mechanical response of the



Proposed Speed Control

Figure 27

turbines. It is not practical to have a control system which would place excessive demands on the prime mover supplying the power to the generator which feeds the cycloconverter. The motor now could never be pulled out of step. If the load torque continuously exceeds the pull-out torque of the motor, the rotor and stator field will slow together to dead stop, yet maximum available torque will still be applied to the shaft by the motor at a frequency of 0 hertz.

This total propulsion control system, incorporated into a system having the previously stated advantages of superconductors in the fields of the generator and the synchronous motor would thus yield a highly competitive propulsion system for large naval vessels.¹ It not only can meet the design specifications for weight and size for a given power rating, but in addition it gives the naval engineer added flexibility in ship design. The naval engineer is no longer hampered by the restraint of placing all of the key propulsion units in direct line of the propellor shafts. Finally, the proposed cycloconverter system gives the added

advantages of fast response and positive control of the shaft position and speed under all load conditions. All of these reasons combine to make this system advantageous for future development.

Appendix A

Derivations

To determine the equations representing the voltage and current across the loads discussed in Chapter I, the following systematic steps are shown.

$$\begin{aligned}
 (1.1.1) \quad E_{d.c.} &= \int_0^{\pi} \frac{1}{T} E(\omega t) d(\omega t) \\
 &= \int_0^{2\pi} \frac{1}{2\pi} E \sin \omega t d(\omega t) \\
 &= \frac{1}{2\pi} \left[\int_0^{\pi} E \sin \omega t d(\omega t) + \int_{\pi}^{2\pi} 0 d(\omega t) \right] \\
 &= \frac{E}{2\pi} \left[-\cos \omega t \right]_0^{\pi} \\
 &= \frac{E}{\pi}
 \end{aligned}$$

$$\begin{aligned}
 (1.1.3) \quad I_{RMS} &= \frac{1}{R} \left[\frac{1}{2\pi} \int_0^{\pi} E^2 \sin^2 \omega t d(\omega t) \right]^{1/2} \\
 &= \frac{E}{R} \left[\frac{1}{2\pi} \left(-\frac{1}{2} \cos \omega t \sin \omega t + \frac{\omega t}{2} \right) \Big|_0^{\pi} \right]^{1/2} \\
 &= \frac{E}{R} \left[\frac{1}{2\pi} \left(\frac{\omega t}{2} - \frac{\sin 2\omega t}{4} \right) \Big|_0^{\pi} \right]^{1/2} \\
 &= \frac{E}{R} \left[\frac{1}{2\pi} \left(\frac{\pi}{2} \right) \right]^{1/2} \\
 &= \frac{E}{2R}
 \end{aligned}$$

$$\begin{aligned}
 (1.1.4) \quad E_{d.c.} &= \int_0^{\pi} \frac{1}{\pi} E \sin \omega t \, d(\omega t) \\
 &= \frac{E}{\pi} \left[-\cos \omega t \right]_0^{\pi} \\
 &= \frac{2E}{\pi}
 \end{aligned}$$

$$\begin{aligned}
 (1.1.5) \quad I_{RMS} &= \frac{1}{R} \left[\frac{1}{\pi} \int_0^{\pi} E^2 \sin^2 \omega t \, d(\omega t) \right] \\
 &= \frac{E}{R} \left[\frac{1}{\pi} \left(\frac{\omega t}{2} - \frac{\sin 2\omega t}{4} \right) \right]_0^{\pi} \\
 &= \frac{E}{R} \left[\frac{1}{\pi} \left(\frac{\pi}{2} \right) \right] \\
 &= \frac{E \sqrt{2}}{2R}
 \end{aligned}$$

$$\begin{aligned}
 (1.1.6) \quad E_{d.c.} &= \int_0^{\pi} \frac{1}{T} E(\omega t) \, d(\omega t) \\
 &= \int_0^{2\pi} \frac{1}{2\pi} E \sin \omega t \, d(\omega t) \\
 &= \frac{E}{2\pi} \left[\int_0^{\alpha} 0 \, d(\omega t) + \int_{\alpha}^{\pi} \sin \omega t \, d(\omega t) + \int_{\pi}^{2\pi} 0 \, d(\omega t) \right] \\
 &= \frac{E}{2\pi} \left[-\cos \omega t \right]_{\alpha}^{\pi} \\
 &= \frac{E}{2\pi} [1 + \cos \alpha]
 \end{aligned}$$

$$\begin{aligned}
 (1.1.7) \quad I_{RMS} &= \frac{1}{R} \left[\frac{1}{2\pi} \int_{\alpha}^{\pi} E^2 \sin^2 \omega t \, d(\omega t) \right]^{1/2} \\
 &= \frac{E}{R} \left[\frac{1}{2\pi} \left(\frac{\omega t}{2} - \frac{\sin 2\omega t}{4} \right) \right]_{\alpha}^{\pi}^{1/2} \\
 &= \frac{E}{R} \left[\frac{1}{2\pi} \left(\frac{\pi}{2} - \frac{\alpha}{2} + \frac{\sin 2\alpha}{4} \right) \right]^{1/2} \\
 &= \frac{E}{2R/\pi} \left(\pi - \alpha + \frac{\sin 2\alpha}{2} \right)^{1/2}
 \end{aligned}$$

$$\begin{aligned}
 (1.1.10) \quad E_{d.c.} &= \int_0^{\pi} \frac{1}{T} E(\omega t) d(\omega t) \\
 &= \int_{\alpha}^{\pi+\alpha} \frac{1}{\pi} E \sin \omega t d(\omega t) \\
 &= \frac{E}{\pi} \left(-\cos \omega t \Big|_{\alpha}^{\pi+\alpha} \right) \\
 &= \frac{E}{\pi} (\cos \alpha + \cos \alpha) \\
 &= \frac{2E}{\pi} \cos \alpha
 \end{aligned}$$

$$\begin{aligned}
 (1.2.1) \quad E_{d.c.} &= \int_{\alpha}^{\alpha+2} \frac{1}{T} E(\omega t) d(\omega t) \\
 &= \frac{3}{2\pi} \int_{\pi/6}^{5\pi/6} E \sin \omega t d(\omega t) \\
 &= \frac{3E}{2\pi} \left(-\cos \omega t \Big|_{\pi/6}^{5\pi/6} \right) \\
 &= \frac{3\sqrt{3}E}{2\pi}
 \end{aligned}$$

$$\begin{aligned}
 (1.2.2) \quad E_{d.c.} &= \frac{3E}{2\pi} \int_{\alpha+\pi/6}^{\alpha+5\pi/6} \sin \omega t d(\omega t) \\
 &= \frac{3E}{2\pi} \left[\cos \left(\frac{\pi}{6} - \alpha \right) + \cos \left(\frac{\pi}{6} + \alpha \right) \right] \\
 &= \frac{3E}{2\pi} \left[2 \cos \left(\frac{\pi}{6} \right) \cos \alpha \right] \\
 &= \frac{3\sqrt{3}E}{2\pi} \cos \alpha
 \end{aligned}$$

$$\begin{aligned}
 (1.2.3) \quad E_{d.c.} &= \frac{3E}{2\pi} \int_{\alpha+\pi/6}^{\pi} \sin \omega t d(\omega t) \\
 &= \frac{3E}{2\pi} \left[-\cos \pi + \cos \left(\alpha + \frac{\pi}{6} \right) \right] \\
 &= \frac{3E}{2\pi} \left[1 + \cos \left(\alpha + \frac{\pi}{6} \right) \right]
 \end{aligned}$$

$$\begin{aligned}
 (1.2.6) \quad E_{d.c.} &= \frac{3E}{\pi} \int_{\pi/3}^{2\pi/3} \sin \omega t \, d(\omega t) \\
 &= \frac{3E}{\pi} \left[-\cos \omega t \right]_{\pi/3}^{2\pi/3} \\
 &= \frac{3E}{\pi} \left(\frac{1}{2} + \frac{1}{2} \right) \\
 &= \frac{3E}{\pi}
 \end{aligned}$$

$$\begin{aligned}
 (1.2.8) \quad E_{d.c.} &= \frac{3E}{\pi} \int_{\alpha + \pi/3}^{\alpha + 2\pi/3} \sin \omega t \, d(\omega t) \\
 &= \frac{3E}{\pi} \left[-\cos \left(\alpha + \frac{2\pi}{3} \right) + \cos \left(\alpha + \frac{\pi}{3} \right) \right] \\
 &= \frac{3E}{\pi} 2 \cos \frac{\pi}{3} \cos \alpha \\
 &= \frac{3E}{\pi} \cos \alpha
 \end{aligned}$$

$$\begin{aligned}
 (1.2.9) \quad E_{d.c.} &= \frac{3E}{\pi} \int_{\alpha + \pi/3}^{\pi} \sin \omega t \, d(\omega t) \\
 &= \frac{3E}{\pi} \left[-\cos \pi + \cos \left(\alpha + \frac{\pi}{3} \right) \right] \\
 &= \frac{3E}{\pi} \left[1 + \cos \left(\alpha + \frac{\pi}{3} \right) \right]
 \end{aligned}$$

$$\begin{aligned}
 (1.2.10) \quad E_{d.c.}' &= \frac{3E}{2\pi} \left[\int_{\pi/6}^{\pi/6 + \mu} \frac{1}{2} (\sin \omega t + \sin (\omega t + \frac{2\pi}{3})) \right. \\
 &\quad \left. + \int_{\pi/6}^{\pi/6} \sin \omega t \right] d(\omega t) \\
 &= \frac{3E}{2\pi} \left[\int_{\pi/6}^{\pi/6 + \mu} \frac{1}{2} \sin \left(\omega t + \frac{\pi}{3} \right) + \int_{\pi/6 + \mu}^{\pi/6} \sin \omega t \right] d(\omega t) \\
 &= \frac{3E}{2\pi} \left[\frac{-\cos}{2} \left(\omega t + \frac{\pi}{3} \right) \right]_{\pi/6}^{\pi/6 + \mu} - \cos \omega t \Big|_{\pi/6 + \mu}^{\pi/6}
 \end{aligned}$$

$$\begin{aligned}
&= \frac{3E}{2\pi} \left[\frac{-1}{2} \cos \left(\frac{\pi}{2} + \mu \right) - \cos \frac{5\pi}{6} + \cos \left(\frac{\pi}{6} + \mu \right) \right] \\
&= \frac{3E}{2\pi} \left[\frac{1}{2} \sin \frac{\pi}{2} \sin \mu + \frac{\sqrt{3}}{2} + \cos \frac{\pi}{6} \cos \mu \right. \\
&\quad \left. - \sin \frac{\pi}{6} \sin \mu \right] \\
&= \frac{3E}{2\pi} \left[\frac{\sin \mu}{2} + \frac{\sqrt{3}}{2} (1 + \cos \mu) - \frac{\sin \mu}{2} \right] \\
&= \frac{3\sqrt{3} E}{2\pi} \cos^2 \left(\frac{\mu}{2} \right) \\
&= E_{d.c.} \cos^2 \left(\frac{\mu}{2} \right)
\end{aligned}$$

$$\begin{aligned}
(1.2.11) \quad E_{d.c.}' &= \frac{3E}{2\pi} \left[\int_{\pi/6+\alpha}^{\pi/6+\alpha+\mu} \frac{1}{2} [\sin \omega t + \sin (\omega t + \frac{2\pi}{3})] \right. \\
&\quad \left. + \int_{\pi/6+\alpha+\mu}^{5\pi/6+\alpha} \sin \omega t \right] d(\omega t) \\
&= \frac{3E}{2\pi} \left[\frac{-1}{2} \cos (\omega t + \frac{\pi}{3}) \Big|_{\pi/6+\alpha}^{\pi/6+\alpha+\mu} - \cos \omega t \Big|_{\pi/6+\alpha+\mu}^{5\pi/6+\alpha} \right] \\
&= \frac{3E}{2\pi} \left[\frac{-1}{2} \cos \left(\frac{\pi}{2} + \alpha + \mu \right) + \frac{1}{2} \cos \left(\frac{\pi}{2} + \alpha \right) \right. \\
&\quad \left. - \cos \left(\frac{5\pi}{6} + \alpha \right) + \cos \left(\frac{\pi}{6} + \alpha + \mu \right) \right] \\
&= \frac{3E}{2\pi} \left[\frac{1}{2} \sin \frac{\pi}{2} \sin (\alpha + \mu) - \frac{1}{2} \sin \frac{\pi}{2} \sin \alpha \right. \\
&\quad \left. - \cos \frac{5\pi}{6} \cos \alpha + \sin \frac{5\pi}{6} \sin \alpha \right. \\
&\quad \left. + \cos \frac{\pi}{6} \cos (\alpha + \mu) - \sin \frac{\pi}{6} \sin (\alpha + \mu) \right] \\
&= \frac{3E}{2\pi} \left[\frac{\sin (\alpha + \mu)}{2} - \frac{\sin \alpha}{2} + \frac{\sqrt{3} \cos \alpha}{2} \right. \\
&\quad \left. + \frac{\sin \alpha}{2} + \frac{\sqrt{3} \cos (\alpha + \mu)}{2} - \frac{\sin (\alpha + \mu)}{2} \right]
\end{aligned}$$

$$\begin{aligned}
&= \frac{3\sqrt{3} E}{2\pi} \frac{\cos \alpha + \cos (\alpha + \mu)}{2} \\
&= E_{\text{d.c.}} \frac{\cos \alpha + \cos (\alpha + \mu)}{2}
\end{aligned}$$

(1.4.4) If $V_L = k \cos \omega_L t$
and $V_S = \frac{-1}{2\pi} \omega_S t$

then:

$$\begin{aligned}
\alpha &= -2k\pi \cos \omega_L t \\
\cos \alpha &= \sin (2k\pi \cos \omega_L t)
\end{aligned}$$

Appendix B

Settings

Oscilloscope settings for photographs of waveforms.

B. 1 Figure 22 Voltage across a resistive load.

Voltage	100 v/cm
Time	20 ms/cm
Frequency	1.5 hertz

B. 2 Figure 23 Firing pulses to thyristors I - IV.

Voltage	5 v/cm
Time	50 ms/cm
Frequency	1.5 hertz

B. 3 Figure 24 Voltage and current in inductive load.

Voltage	100 v/cm
Current	.5 a/cm
Time	10 ms/cm
Frequency	6 hertz

B. 4 Figure 25 Voltage across stator winding.

Figure 25a.

Voltage	100 v/cm
Time	20 ms/cm
Frequency	6 hertz

Figure 25b.

Voltage	100 v/cm
Time	20 ms/cm
Frequency	15 hertz

REFERENCES

1. Greene, David L., Analysis of a Marine Propulsion System Incorporating Superconducting Electrical Machinery, M.I.T. Thesis Ph.D., 1970.
2. Marti, O. K., and Winograd, H., Mercury Arc Rectifiers, McGraw-Hill: New York. 1930.
3. Rissik, H., The Fundamental Theory of Arc Converters, Chapman: London. 1939.
4. Gentry, F. E., et. al., Semiconductor Controlled Rectifiers, Prentice-Hall: Englewood Cliffs. 1964.
5. Kusko, A., Solid-State DC Motor Drivers, M.I.T. Press: Cambridge. 1969.
6. Bland, R. J., "Factors Affecting the Operation of a Phase-Controlled Cycloconverter", Proceedings of the IEE, Vol. 114, No. 12, December 1967, pp. 1908-1916.
7. Wickes, W. E., Logic Design with Integrated Circuits, Wiley: New York. 1968
8. Fitzgerald, A. E., and Kingsley, C., Electric Machinery, McGraw-Hill: New York. 1961.
9. Pappenfus, E. W., Bruene, W. B., and Schoenike, E. O., Single Sideband Principles and Circuits, McGraw-Hill: New York. 1964.

Thesis
S4058

Sears

119250

An SCR cycloconverter
for a cryogenic pro-
pulsion system.

18 NOV 70

DISPLAY

Thesis
S4058

Sears

119250

An SCR cycloconverter
for a cryogenic pro-
pulsion system.

thes4058

An SCR cycloconverter for a cryogenic pr



3 2768 000 99589 8

DUDLEY KNOX LIBRARY